

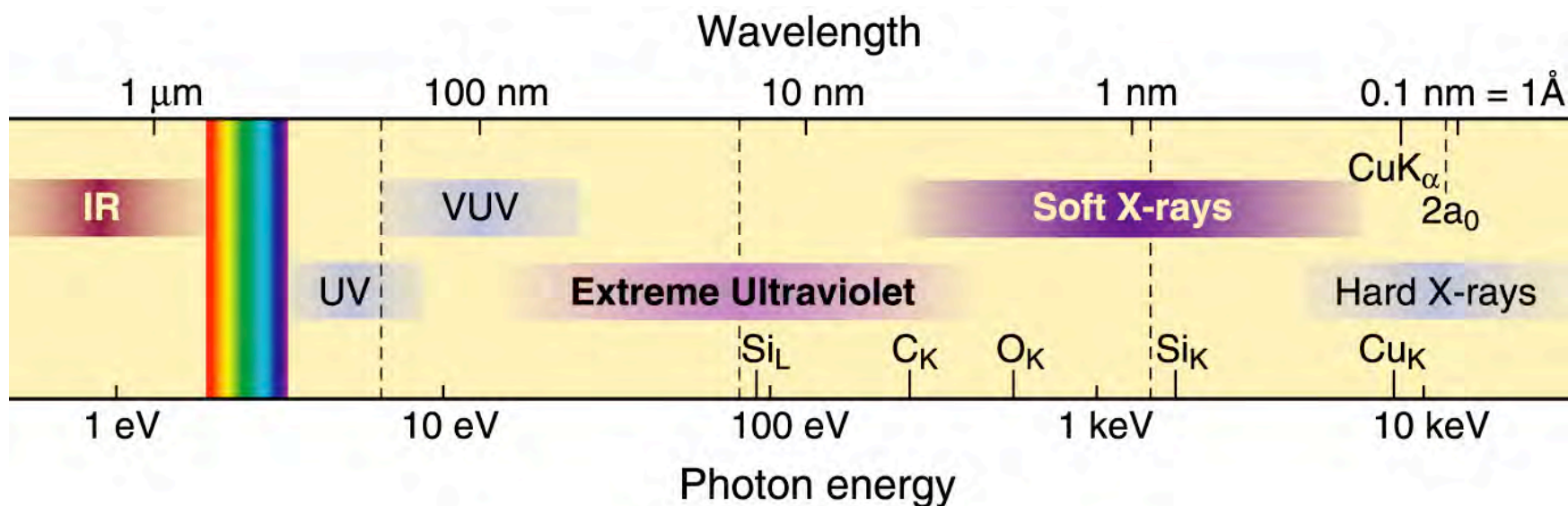


EUV and Soft X-Ray Optics

David Attwood
University of California, Berkeley
and
Advanced Light Source, LBNL

Cheiron School
October 2010
SPRING-8

The short wavelength region of the electromagnetic spectrum



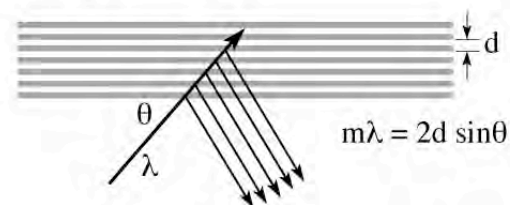
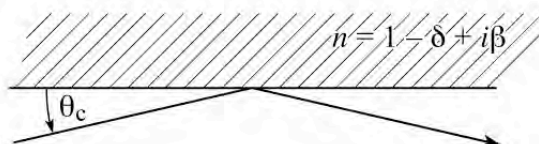
- See smaller features
- Write smaller patterns
- Elemental and chemical sensitivity

$$\hbar\omega \cdot \lambda = hc = 1239.842 \text{ eV nm}$$

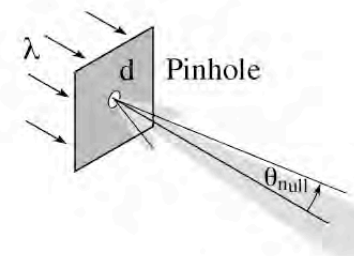
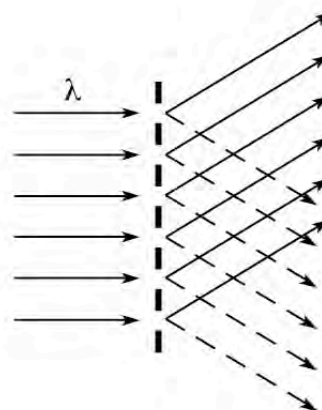
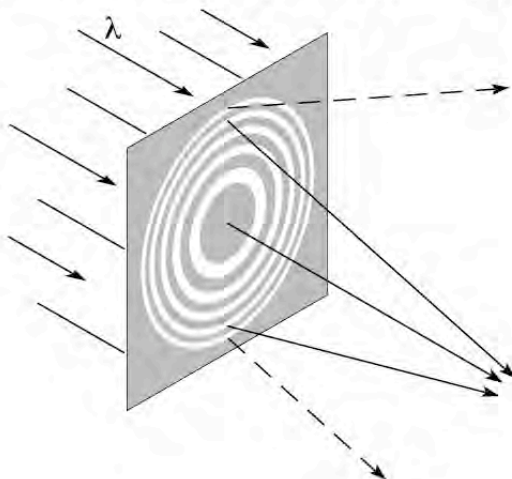
$$n = 1 - \delta + i\beta \quad \delta, \beta \ll 1$$

Available x-ray optical techniques

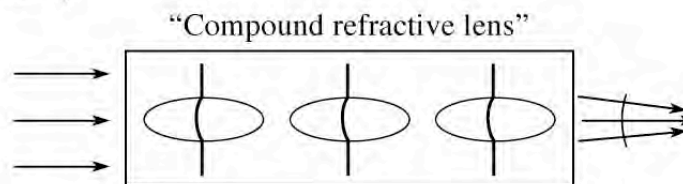
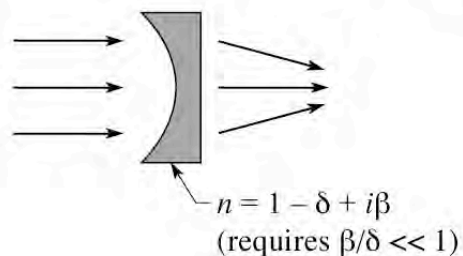
- Reflection (glancing incidence or multilayer coatings)



- Diffraction (zone plates, gratings, pinholes)



- Refraction (only for hard x-rays, > 20 keV)



A. Snigerev et al., *Nature* 384, 49 (7Nov.1996)

B. Lengeler et al., *J. Appl. Phys.* 84, 5855 (1Dec.1998)

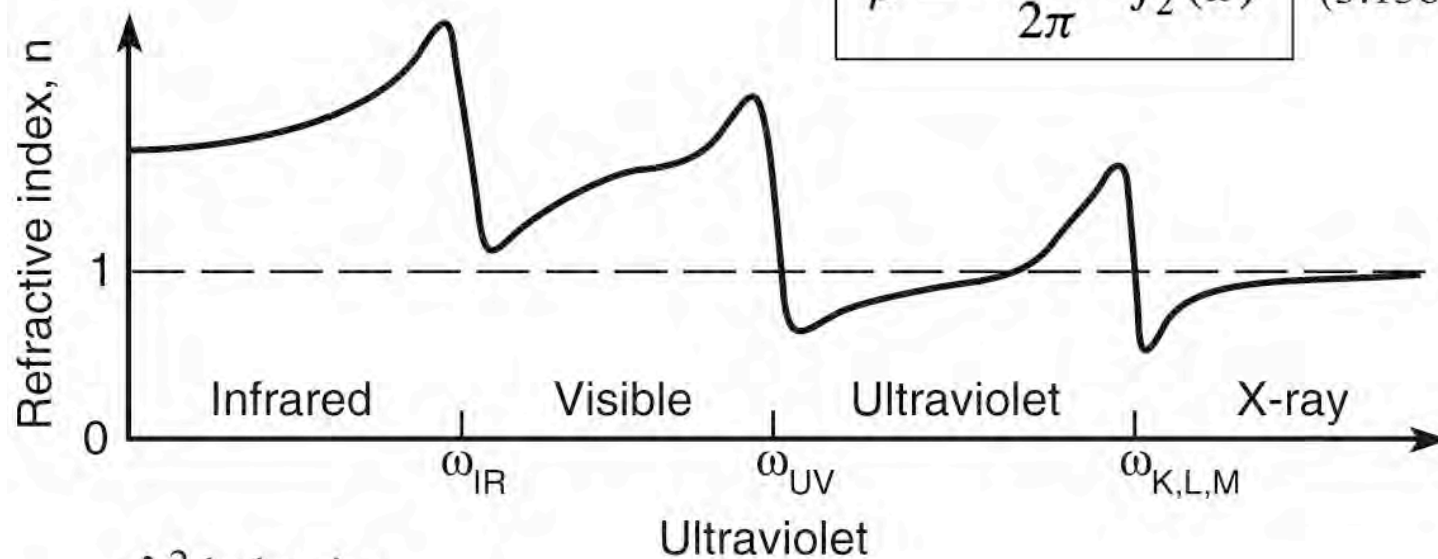
AvailOpticTechSXR@UVAi

Refractive index from the IR to x-ray spectral region

$$n(\omega) = 1 - \delta + i\beta \quad (3.12)$$

$$\delta = \frac{n_a r_e \lambda^2}{2\pi} f_1^0(\omega) \quad (3.13a)$$

$$\beta = \frac{n_a r_e \lambda^2}{2\pi} f_2^0(\omega) \quad (3.13b)$$



- λ^2 behavior
- δ & $\beta \ll 1$
- δ -crossover

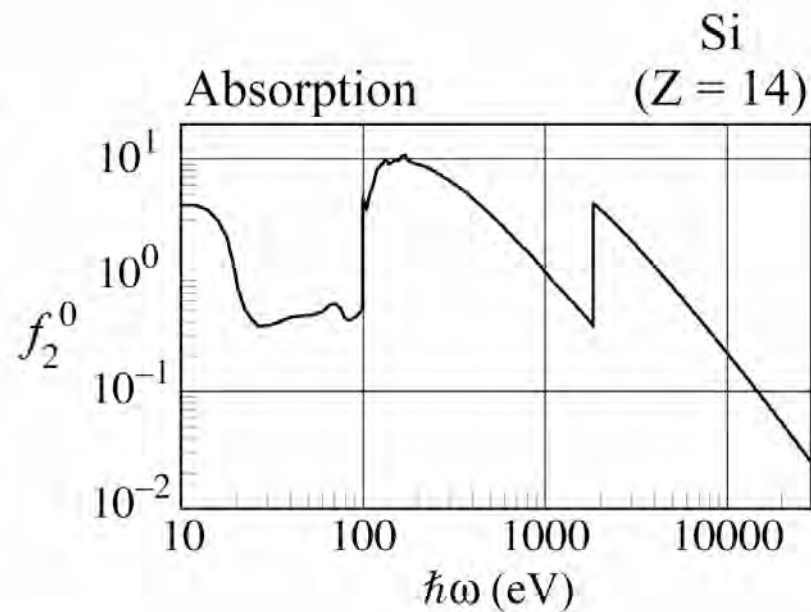
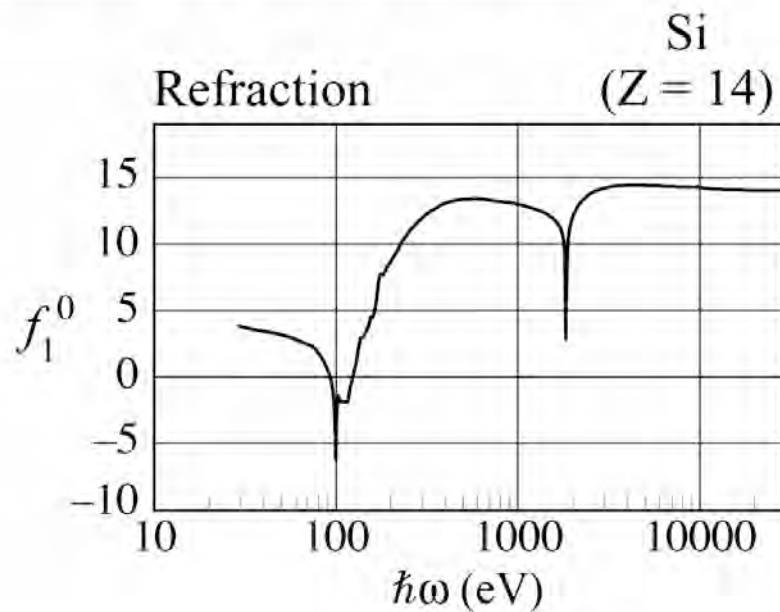
Ch03_RefrIndxIR.XR.ai

Refractive index at nanometer wavelengths

Refractive Index

$$n = 1 - \delta + i\beta = 1 - \frac{n_a r_e \lambda^2}{2\pi} (f_1^0 - i f_2^0)$$

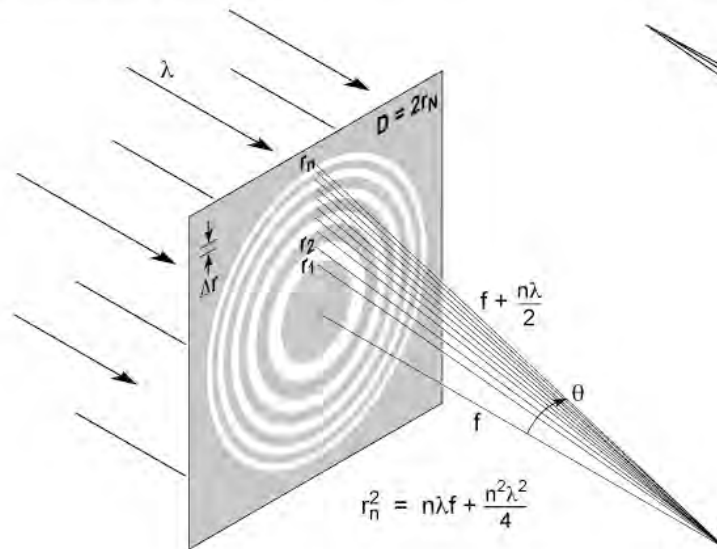
Atomic scattering factors



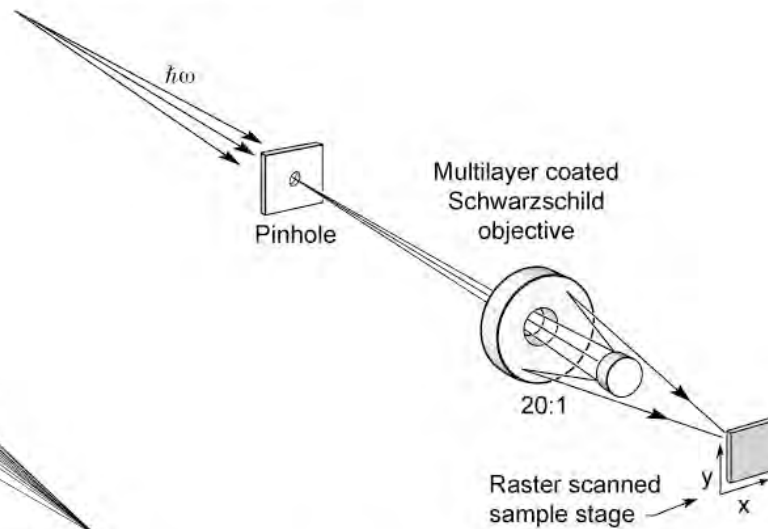
ScattmgRefracIndex_June2009.ai

Diffractive and reflective optics for EUV, soft x-rays and hard x-rays

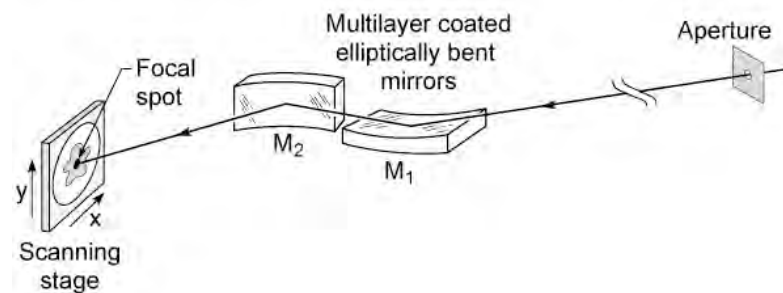
a) Fresnel zone plate



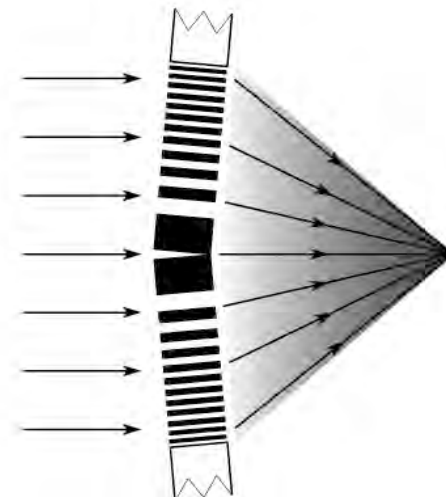
b) Schwarzschild objective



c) Kirkpatrick-Baez mirror pair

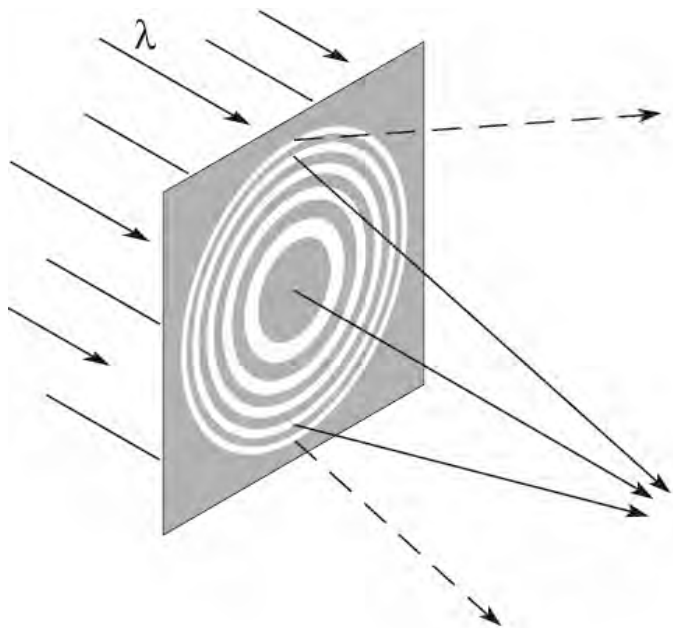


d) Multilayer Laue lens

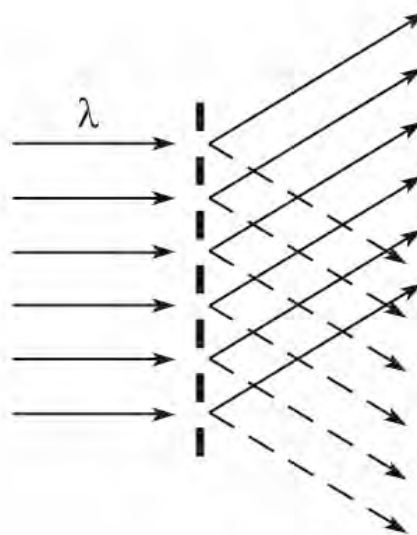


Diffractive optics for soft x-rays and EUV

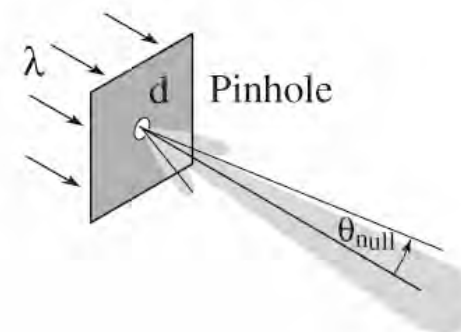
Zone Plates



Gratings

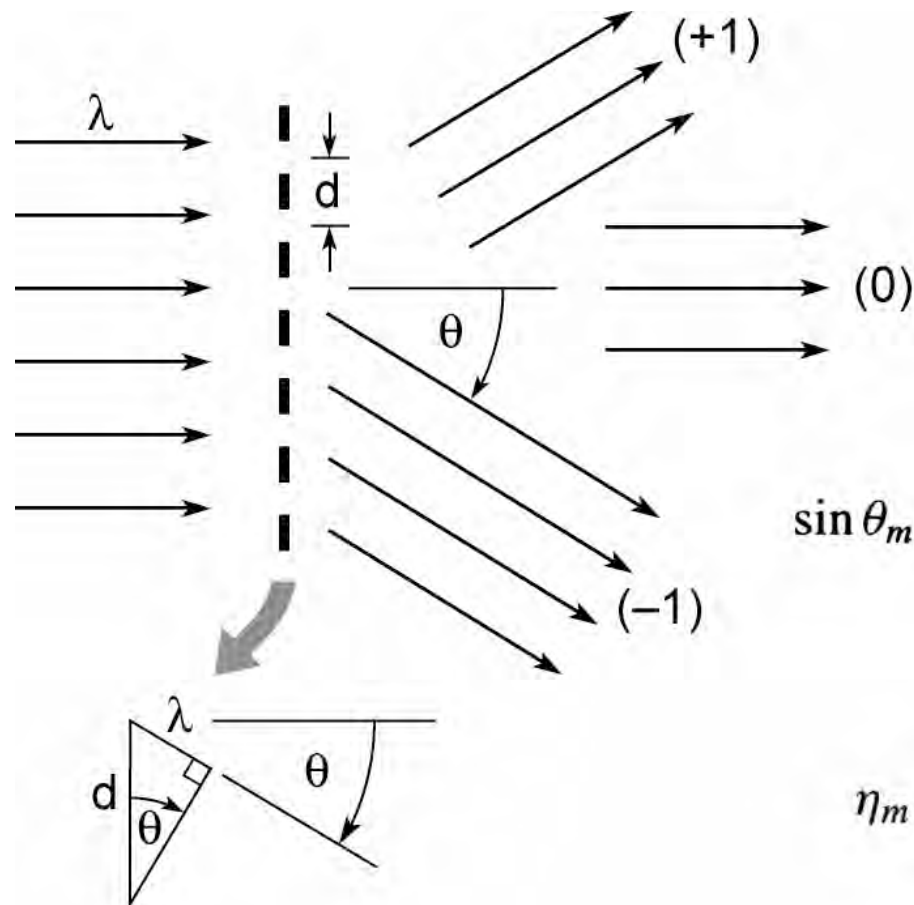


Pinholes



DiffraOptics.ai

Diffraction from a transmission grating



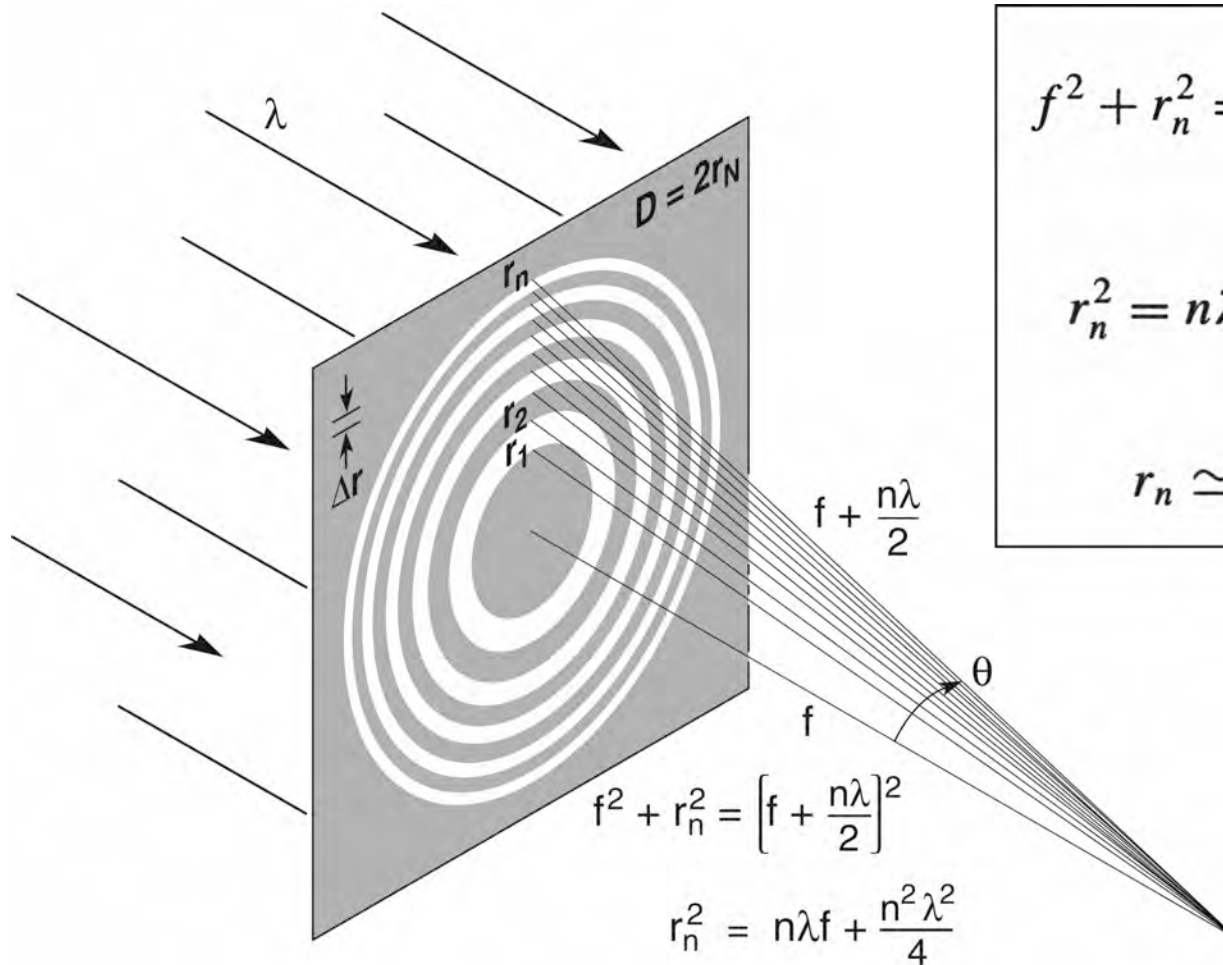
$$\sin \theta_m = \frac{m\lambda}{d} ; \quad m = 0, \pm 1, \pm 2, \pm 3, \dots \quad (9.2)$$

$$\eta_m = \begin{cases} \frac{1}{4} & m = 0 \\ 1/m^2\pi^2 & m \text{ odd} \\ 0 & m \text{ even} \end{cases} \quad (9.24)$$

(50% absorbed)

Ch09_F03VGrev.4.04.ai

A Fresnel zone plate lens

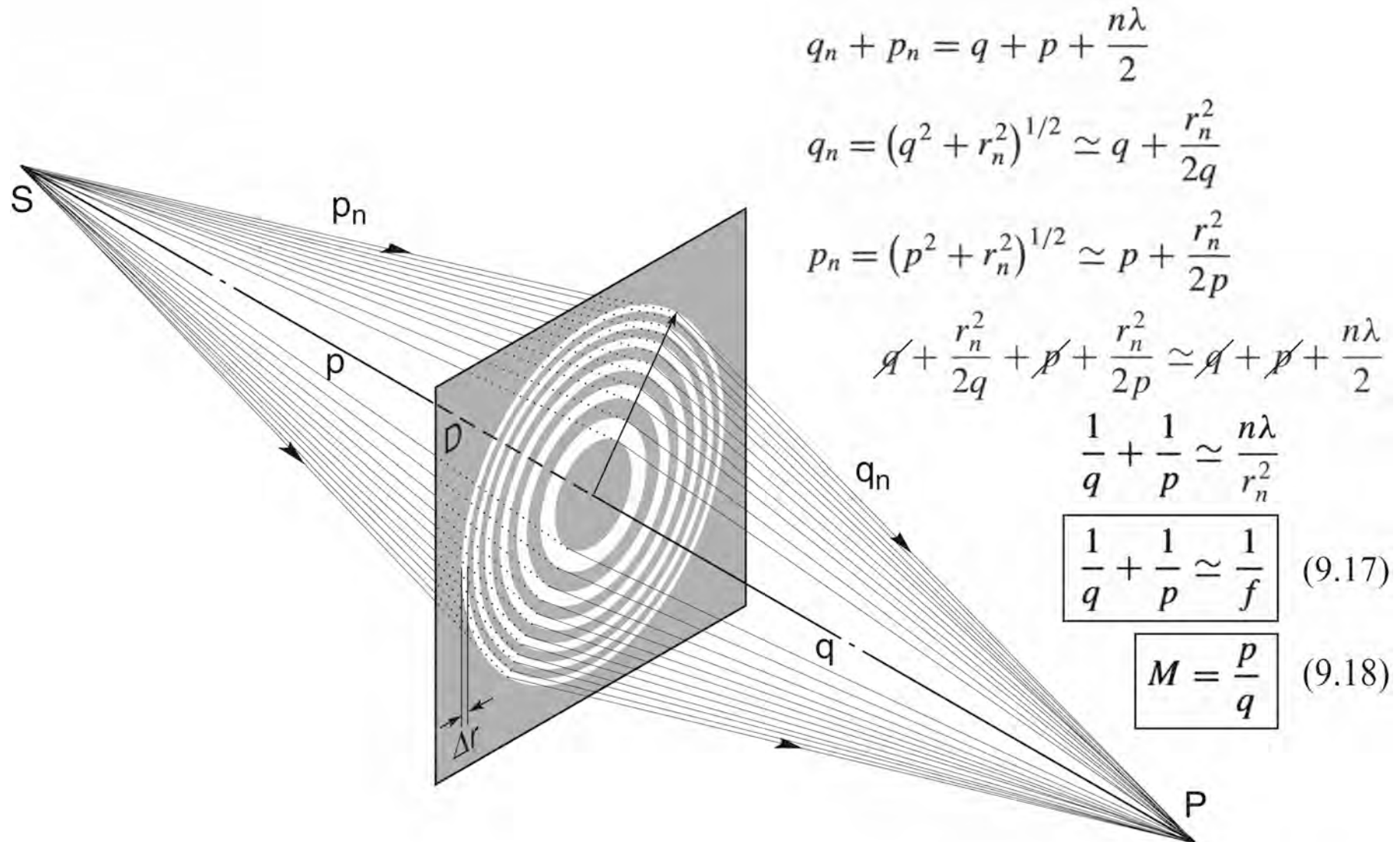


$$f^2 + r_n^2 = \left(f + \frac{n\lambda}{2}\right)^2 \quad (9.8)$$

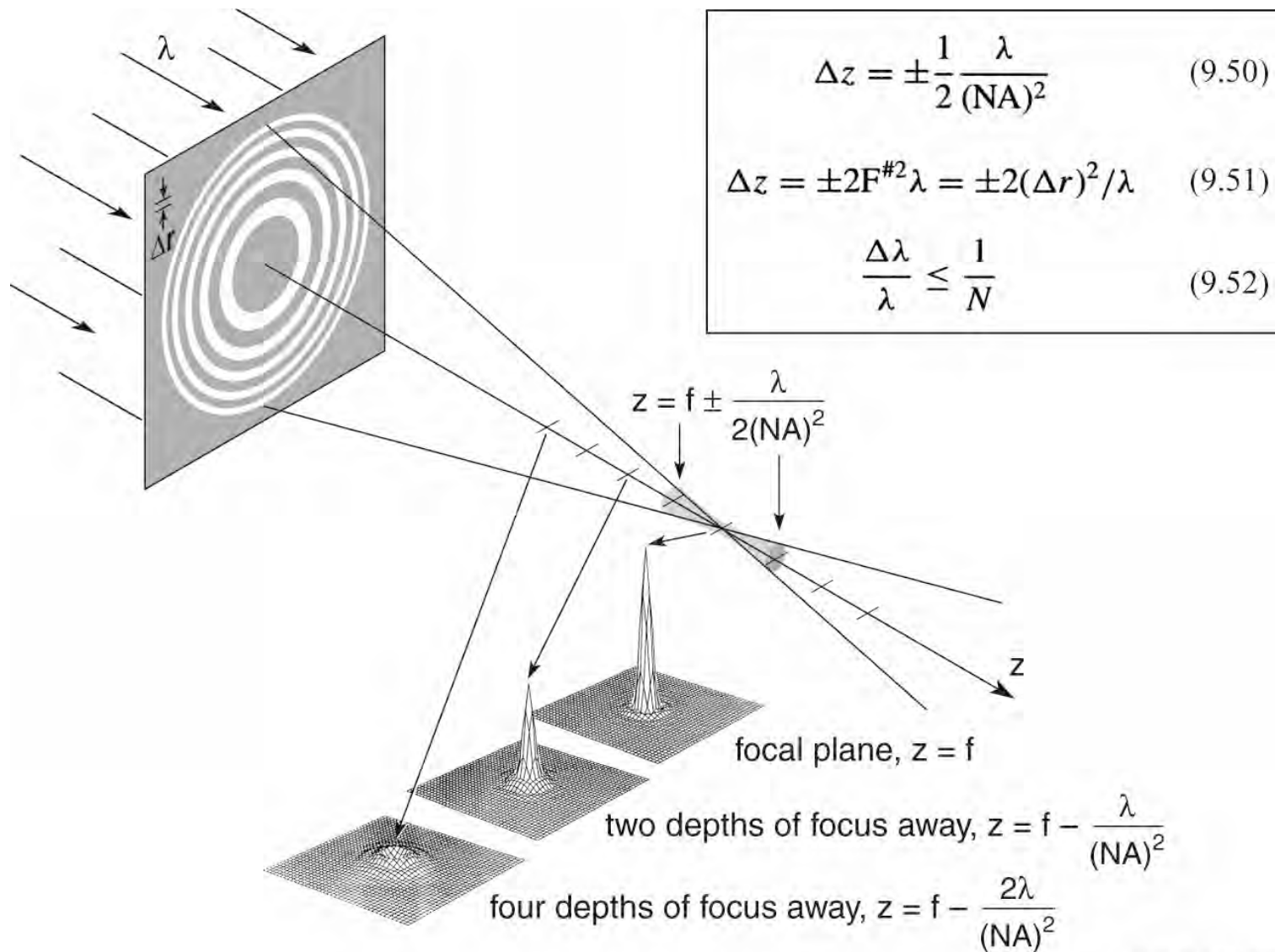
$$r_n^2 = n\lambda f + \frac{n^2\lambda^2}{4} \quad (9.9)$$

$$r_n \simeq \sqrt{n\lambda f} \quad (9.10)$$

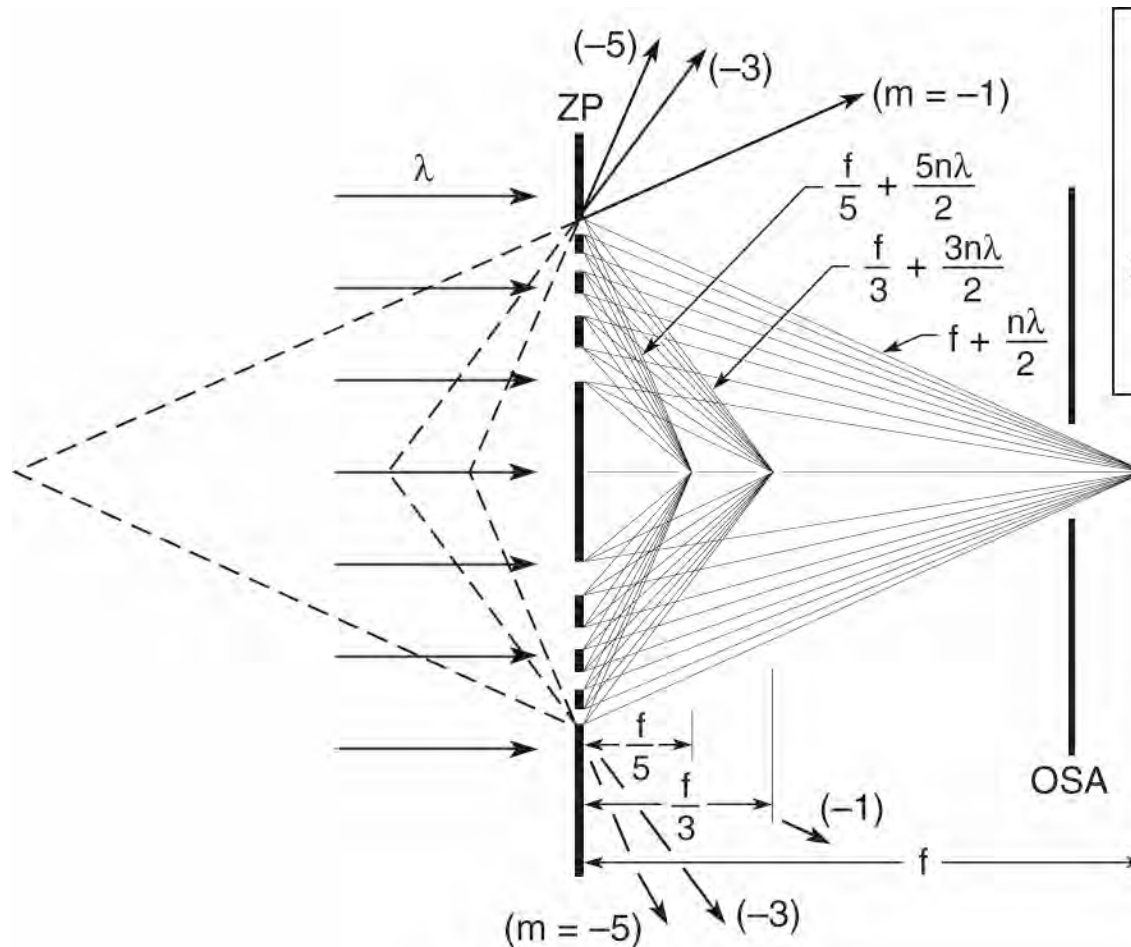
A Fresnel zone plate lens used as a diffractive lens for point to point imaging



Depth of focus and spectral bandwidth



Zone plate diffractive focusing for higher orders

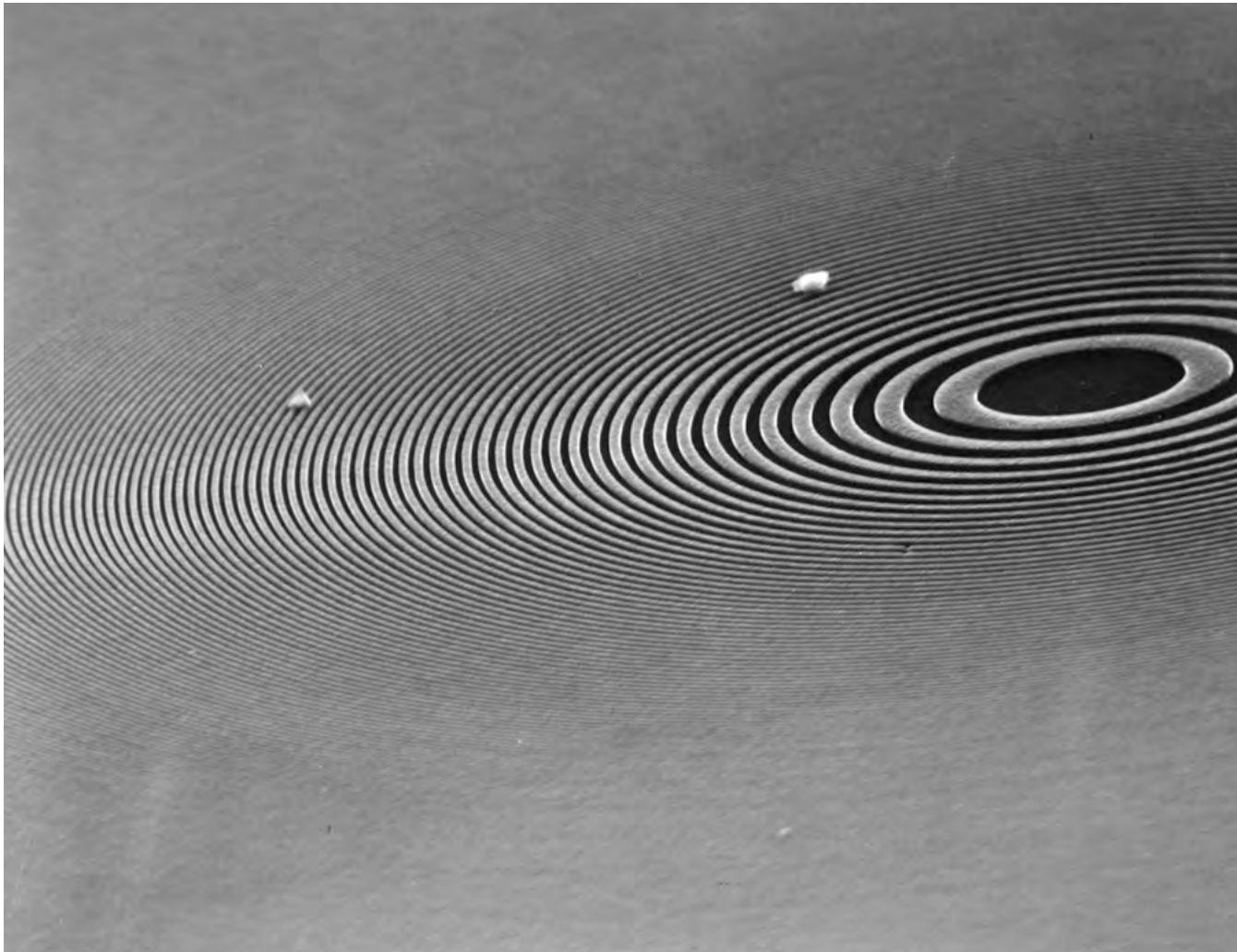


$$r_n^2 \simeq mn\lambda f_m \quad (9.19)$$

$$\eta_m = \begin{cases} \frac{1}{4} & m = 0 \\ 1/m^2\pi^2 & m \text{ odd} \\ 0 & m \text{ even} \end{cases} \quad (9.24)$$

Ch09_F08VG.ai

A Fresnel zone plate lens for soft x-ray microscopy



Courtesy of E. Anderson, LBNL

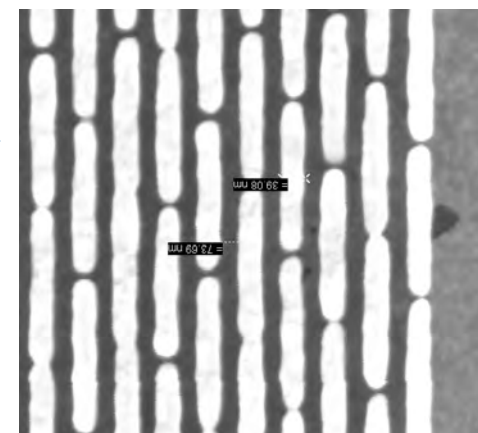


Zone plates for ALS STXM beamlines – “3D Engineered Nanostructures”

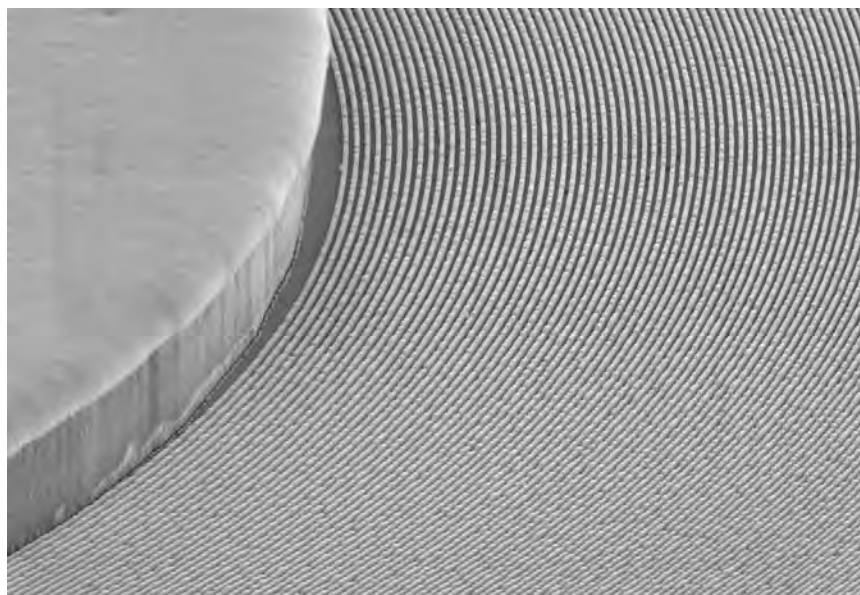


$\Delta r = 35 \text{ nm}$, $\Delta t = 180 \text{ nm Au}$, $N = 1700$
 $D = 240 \text{ }\mu\text{m}$, $3 \times 95 \text{ }\mu\text{m}^D$ central stop

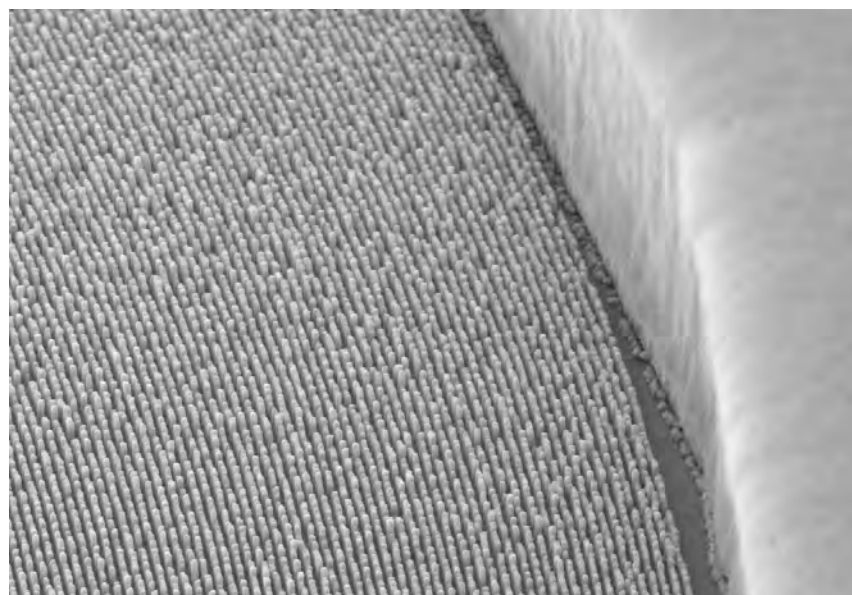
Outer
zone
close-up



Inner zones



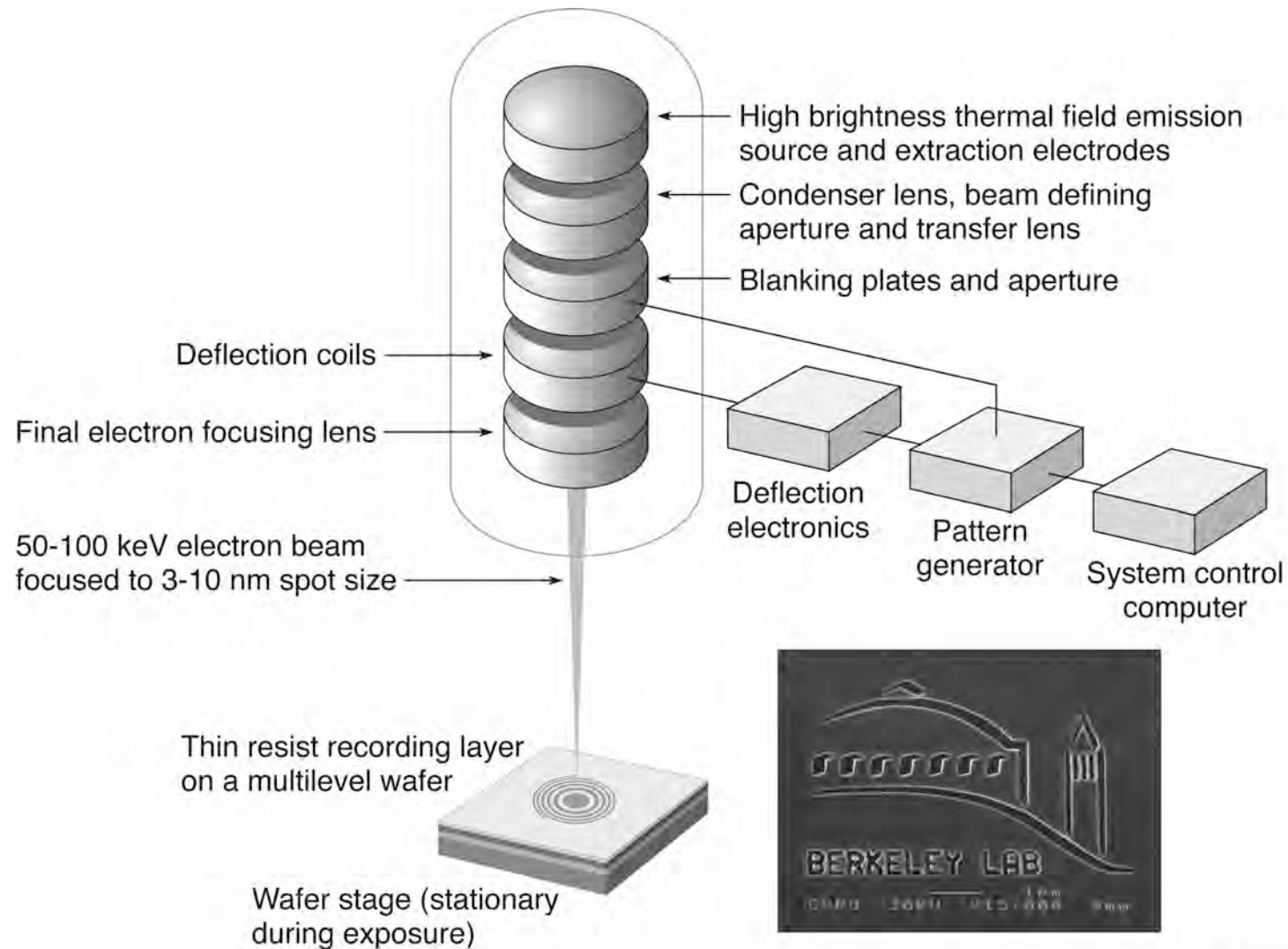
Outer zones



E. Anderson, LBNL



The Nanowriter: high resolution electron beam writing with high placement accuracy

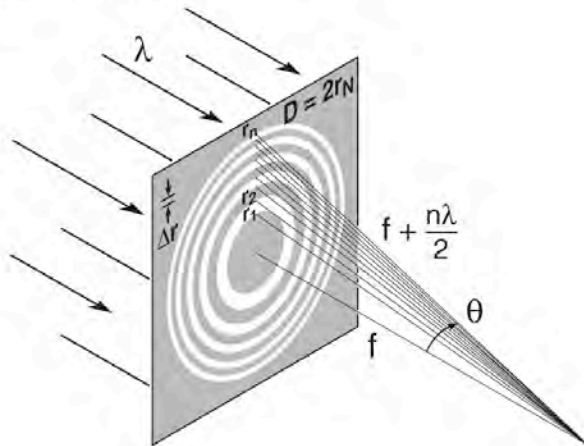


Ch09_F43VG.ai

Courtesy of E. Anderson (LBNL)

Zones plates for soft x-ray image formation

Zone Plate Lens



Zone Plate Formulae

$$r_n^2 = n\lambda f + \frac{n^2\lambda^2}{4} \quad (9.9)$$

$$\lambda = 2.5 \text{ nm},$$

$$\Delta r = 25 \text{ nm}$$

$$N = 618$$

$$D = 4N\Delta r \quad (9.13)$$

$$63 \text{ } \mu\text{m}$$

$$f = \frac{4N(\Delta r)^2}{\lambda} \quad (9.14)$$

$$0.63 \text{ mm}$$

$$NA = \frac{\lambda}{2\Delta r} \quad (9.15)$$

$$0.05$$

$$\text{Res.} = k_1 \frac{\lambda}{NA} = 2k_1\Delta r \begin{cases} k_1 = 0.61 \\ (\sigma = 0) \end{cases} \quad \begin{cases} 1.22\Delta r = 30 \text{ nm} \\ 0.8\Delta r = 19 \text{ nm} \end{cases}$$

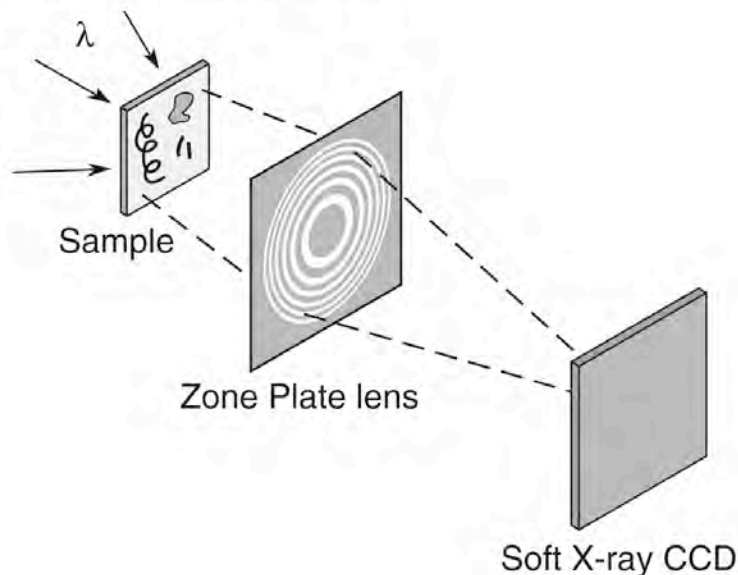
$$\text{DOF} = \pm \frac{1}{2} \frac{\lambda}{(NA)^2} \quad (9.50)$$

$$1 \text{ } \mu\text{m}$$

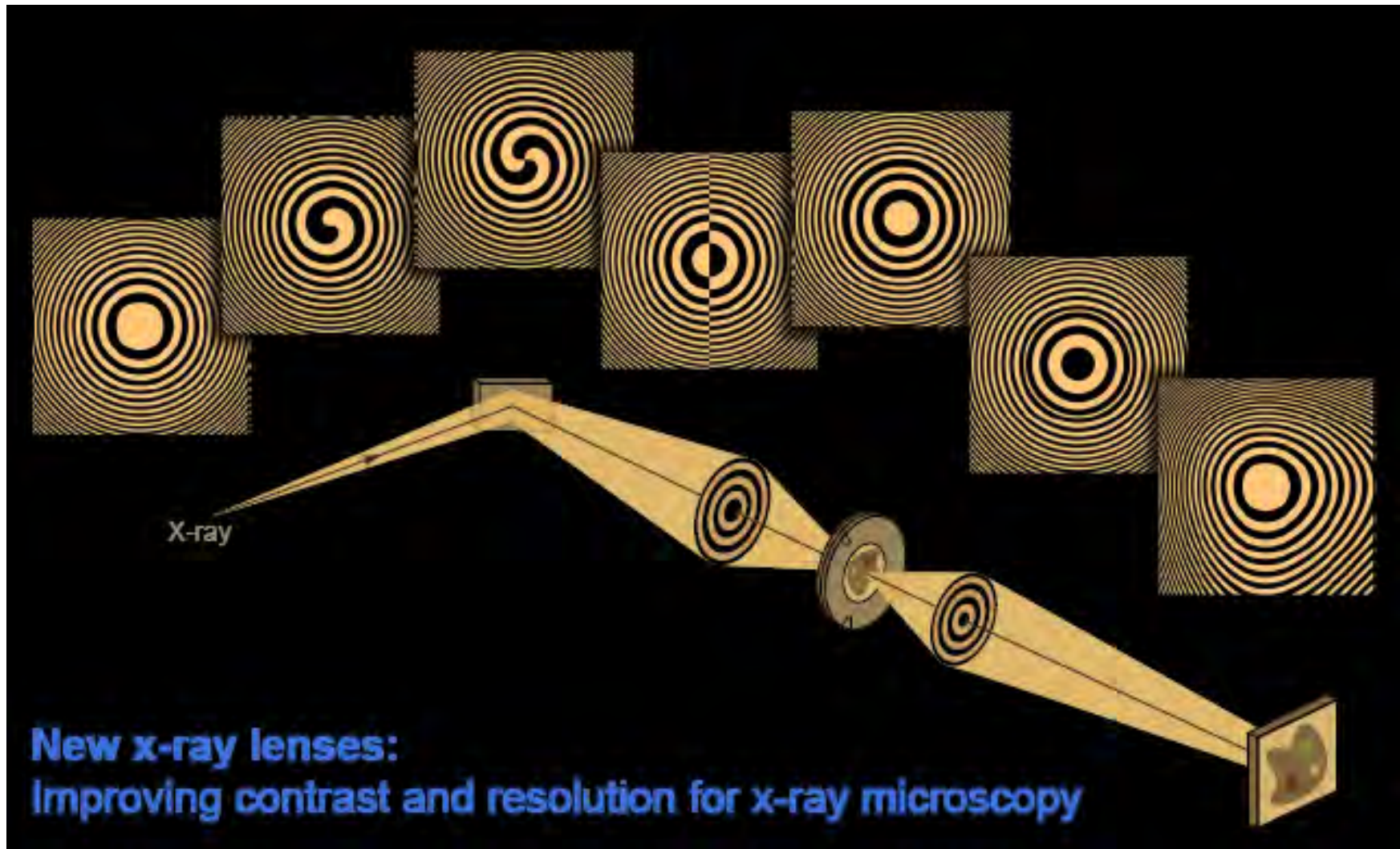
$$\frac{\Delta\lambda}{\lambda} \leq \frac{1}{N} \quad (9.52)$$

$$1/700$$

Soft X-Ray Microscope



New x-ray lenses: Improving contrast and resolution for x-ray microscopy

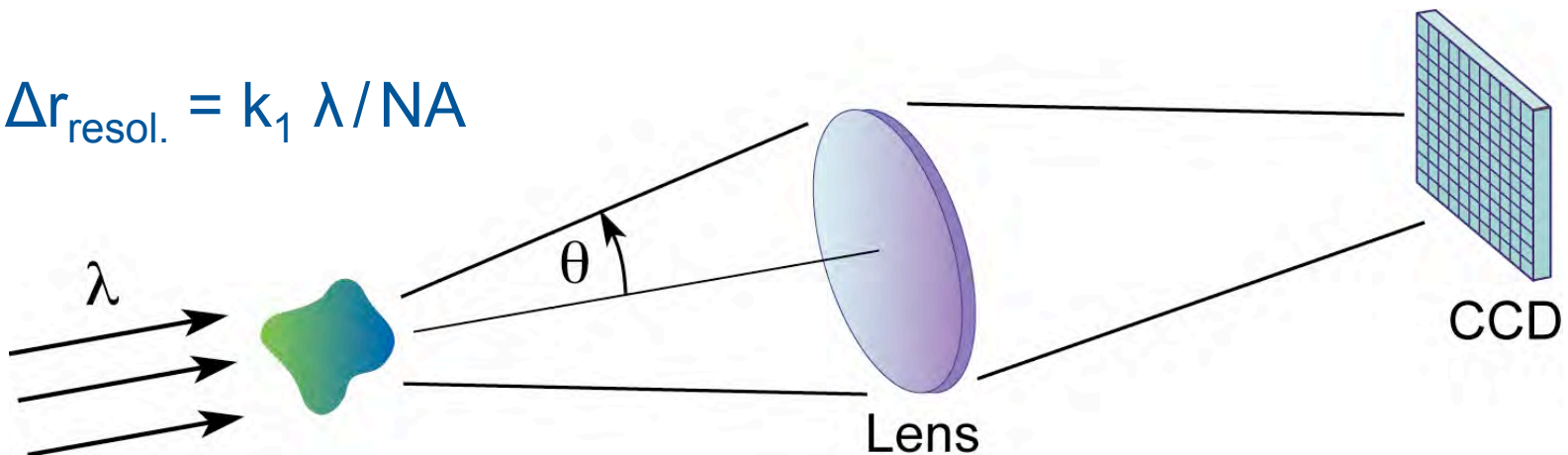


C. Chang, A. Sakdinawat, P.J. Fischer, E.H. Anderson, D.T. Attwood, Opt. Lett. 2006; Sakdinawat and Liu, Opt. Lett. 2007; Sakdinawat and Liu, Opt. Express 2008

Diffraction limited x-ray imaging

Diffraction limited imaging is limited by the finite wavelength and acceptance aperture:

$$\Delta r_{\text{resol.}} = k_1 \lambda / \text{NA}$$



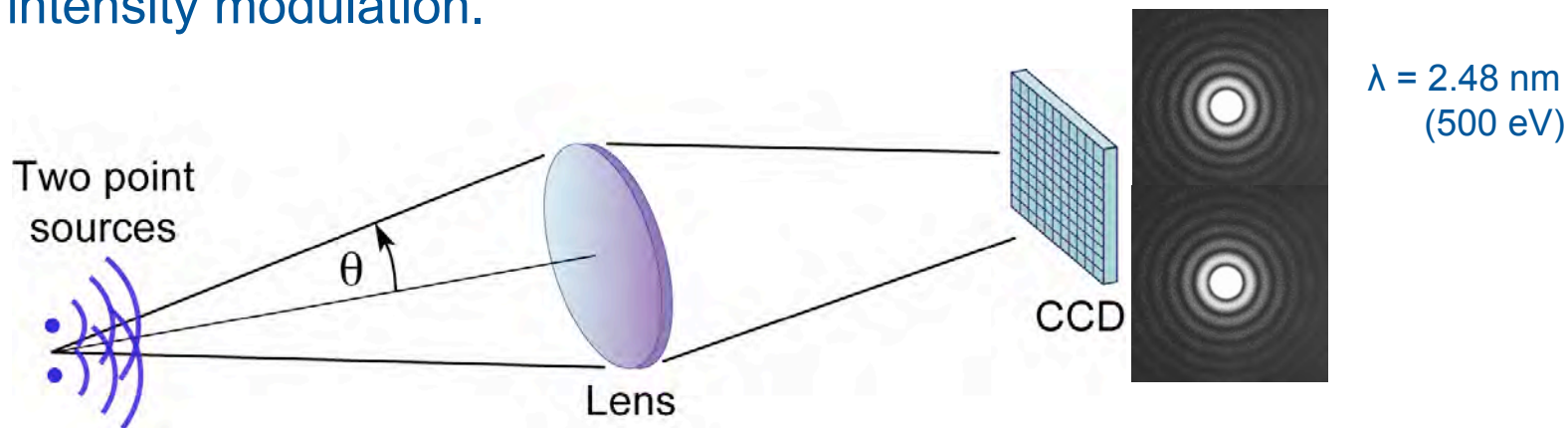
where $\text{NA} = n \sin\theta$ and the constant k_1 depends on illumination and specific image modulation criteria.
For x-rays

$$n = 1 - \delta + i\beta$$

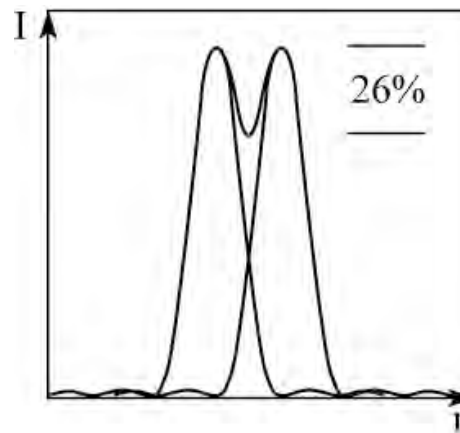
$$\delta, \beta \ll 1$$

Diffraction limited x-ray imaging

For example, the widely accepted Rayleigh criteria for resolving two adjacent, mutually incoherent, point sources of light, results in a 26% intensity modulation.



Two overlapping
Airy patterns



$$\Delta r_{\text{resol.}} = 0.61 \lambda / \text{NA}$$

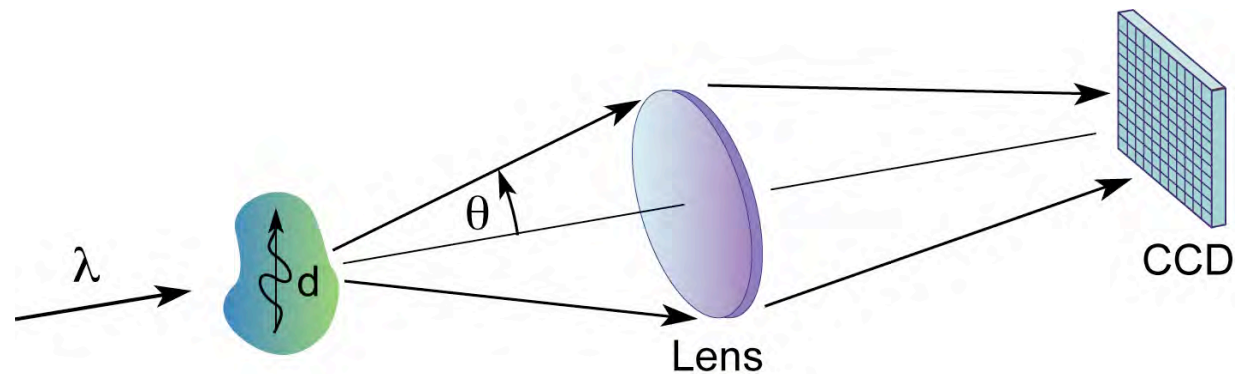
Resultant intensity pattern when the two point sources are “just resolved”, such that the central lobe maximum due to one point source overlaps the first minimum (dark ring) of the other.

Note: Other definitions are possible, depending on the application and the ability to discern separated objects.

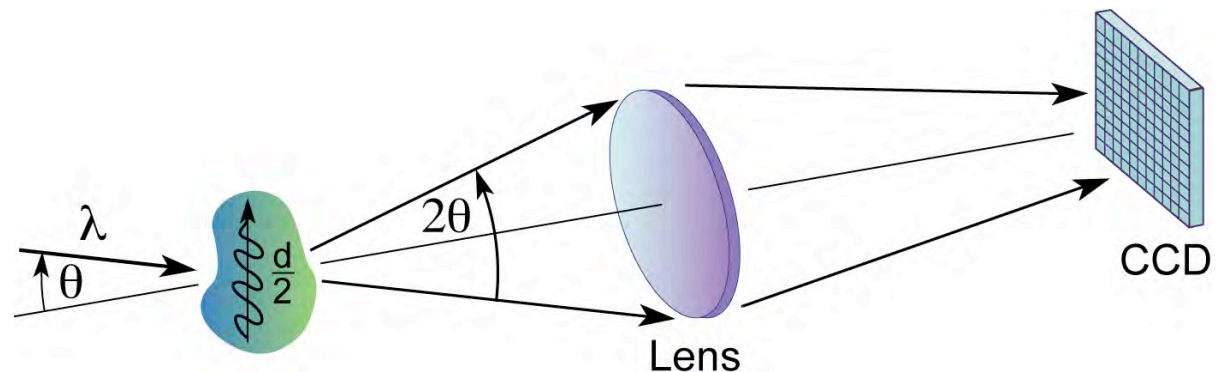
Resolution and illumination

Achievable resolution can be improved by varying illumination:

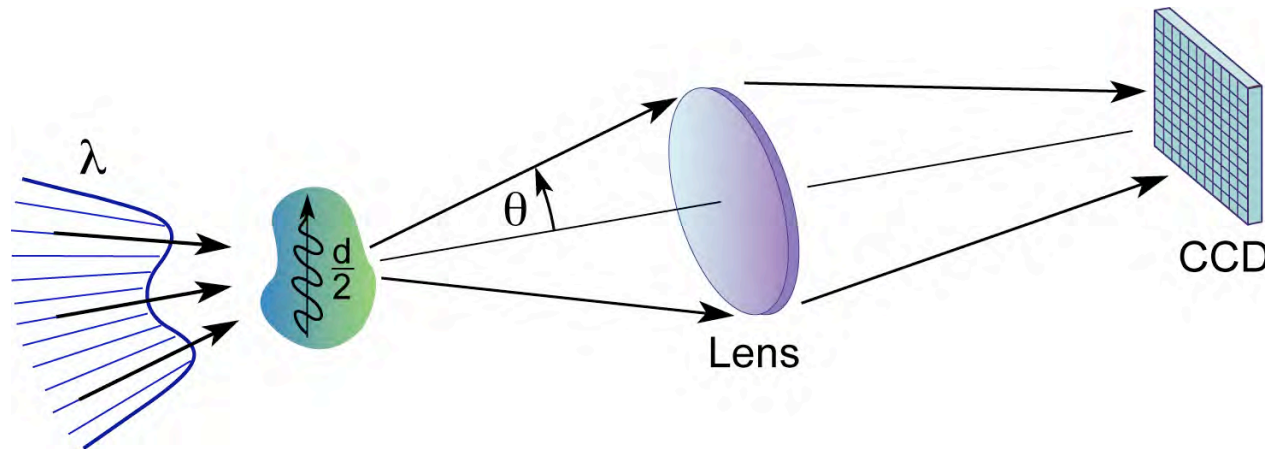
An object pattern of periodicity d diffracts light and is just captured by the lens – setting the diffraction limited resolution limit.



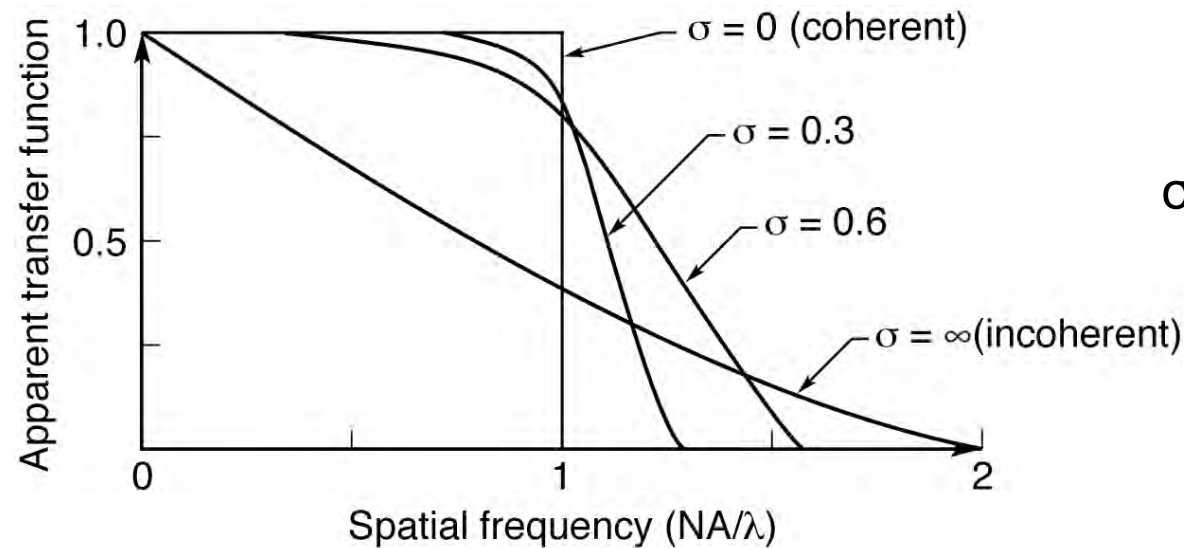
Diffraction from an object of smaller periodicity, $d/2$, is just captured, and resolved, when illuminated from an angle.



Resolution, illumination, and optical transfer function



Spatial frequency response of the optical system can be optimized by tailoring the angular distribution of illumination.



$$\sigma = \frac{NA_{\text{cond}}}{NA_{\text{obj}}} \quad (10.3)$$

LETTERS

Soft X-ray microscopy at a spatial resolution better than 15 nm

Weilun Chao^{1,2}, Bruce D. Harteneck¹, J. Alexander Liddle¹, Erik H. Anderson¹ & David T. Attwood^{1,2}

Analytical tools that have spatial resolution at the nanometre scale are indispensable for the life and physical sciences. It is desirable that these tools also permit elemental and chemical identification on a scale of 10 nm or less, with large penetration depths. A variety of techniques^{1–7} in X-ray imaging are currently being developed that may provide these combined capabilities. Here we report the achievement of sub-15-nm spatial resolution with a soft X-ray microscope—and a clear path to below 10 nm—using an overlay technique for zone plate fabrication. The microscope covers a spectral range from a photon energy of 250 eV (~5 nm wavelength) to 1.8 keV (~0.7 nm), so that primary K and L atomic resonances of elements such as C, N, O, Al, Ti, Fe, Co and Ni can be probed. This X-ray microscopy technique is therefore suitable for a wide range of studies: biological imaging in the water window^{8,9}; studies of wet environmental samples^{10,11}; studies of magnetic nanostructures with both elemental and spin-orbit sensitivity^{12–14}; studies that require viewing through thin windows, coatings or substrates (such as buried electronic devices in a silicon chip¹⁵); and three-dimensional imaging of cryogenically fixed biological cells^{5,16}.

The microscope XM-1 at the Advanced Light Source (ALS) in Berkeley¹⁷ is schematically shown in Fig. 1. The microscope type is similar to that pioneered by the Göttingen/BESSY group (ref. 18, and references therein). A 'micro' zone plate (MZP) projects a full-field image to an X-ray-sensitive CCD (charge-coupled device), typically in one or a few seconds, often with several hundred images per day. The field of view is typically 10 μm , corresponding to a magnification of 2,500. The condenser zone plate (CZP), with a central stop, serves two purposes in that it provides partially coherent hollow-cone illumination², and, in combination with a pinhole, serves as the

monochromator. Monochromatic radiation of $\lambda/\Delta\lambda = 500$ is used. Both zone plates are fabricated in-house, using electron beam lithography¹⁹.

The spatial resolution of a zone plate based microscope is equal to $k_1\lambda/NA_{\text{MZP}}$ where λ is the wavelength, NA_{MZP} is the numerical aperture of the MZP, and k_1 is an illumination dependent constant, which ranges from 0.3 to 0.61. For a zone plate lens used at high magnification, $NA_{\text{MZP}} = \lambda/2\Delta r_{\text{MZP}}$ where Δr_{MZP} is the outermost (smallest) zone width of the MZP²⁰. For the partially coherent illumination^{21,22} used here, $k_1 \approx 0.4$ and thus the theoretical resolution is $0.8\Delta r_{\text{MZP}}$, as calculated using the SPLAT computer program²³ (a two-dimensional scalar diffraction code, which evaluates partially coherent imaging). In previous results with a $\Delta r_{\text{MZP}} = 25$ nm zone plate, we reported² an unambiguous spatial resolution of 20 nm. Here we describe the use of an overlay nanofabrication technique that allows us to fabricate zone plates with finer outer zone widths, to $\Delta r_{\text{MZP}} = 15$ nm, and to achieve a spatial resolution of below 15 nm, with clear potential for further extension.

This technique overcomes nanofabrication limits due to electron beam broadening in high feature density patterning. Beam broadening results from electron scattering within the recording medium (resist), leading to a loss of image contrast and thus resolvability for

$$\lambda = 1.52 \text{ nm (815 eV)}$$

$$\Delta r = 15 \text{ nm}$$

$$N = 500$$

$$D = 30 \mu\text{m}$$

$$f = 300 \mu\text{m}$$

$$\sigma = 0.38$$

$$0.8 \Delta r = 12 \text{ nm}$$

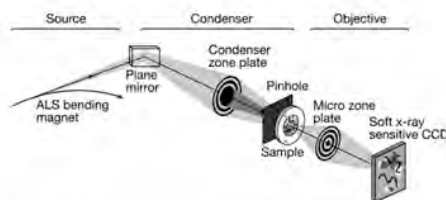


Figure 1 | A diagram of the soft X-ray microscope XM-1. The microscope uses a micro zone plate to project a full field image onto a CCD camera that is sensitive to soft X-rays. Partially coherent, hollow-cone illumination of the sample is provided by a condenser zone plate. A central stop and a pinhole provide monochromatization.

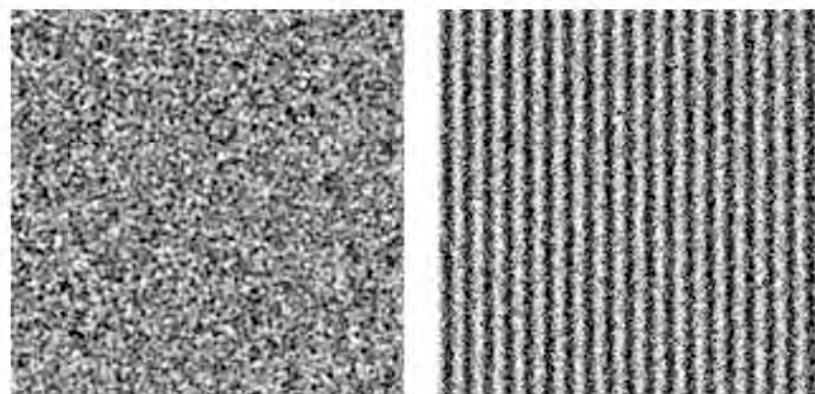


Figure 4 | Soft X-ray images of a 15.1 nm half-period test object, as formed with zone plates having outer zone widths of 25 nm and 15 nm.

Cr/Si test pattern (Cr L₃ @ 574 eV)
(2000 X 2000, 10⁴ ph/pixel)

¹Center for X-ray Optics, Lawrence Berkeley National Laboratory, 1 Cyclotron Road, MS 2-400, ²Department of Electrical Engineering, California, Berkeley, California 94720, USA

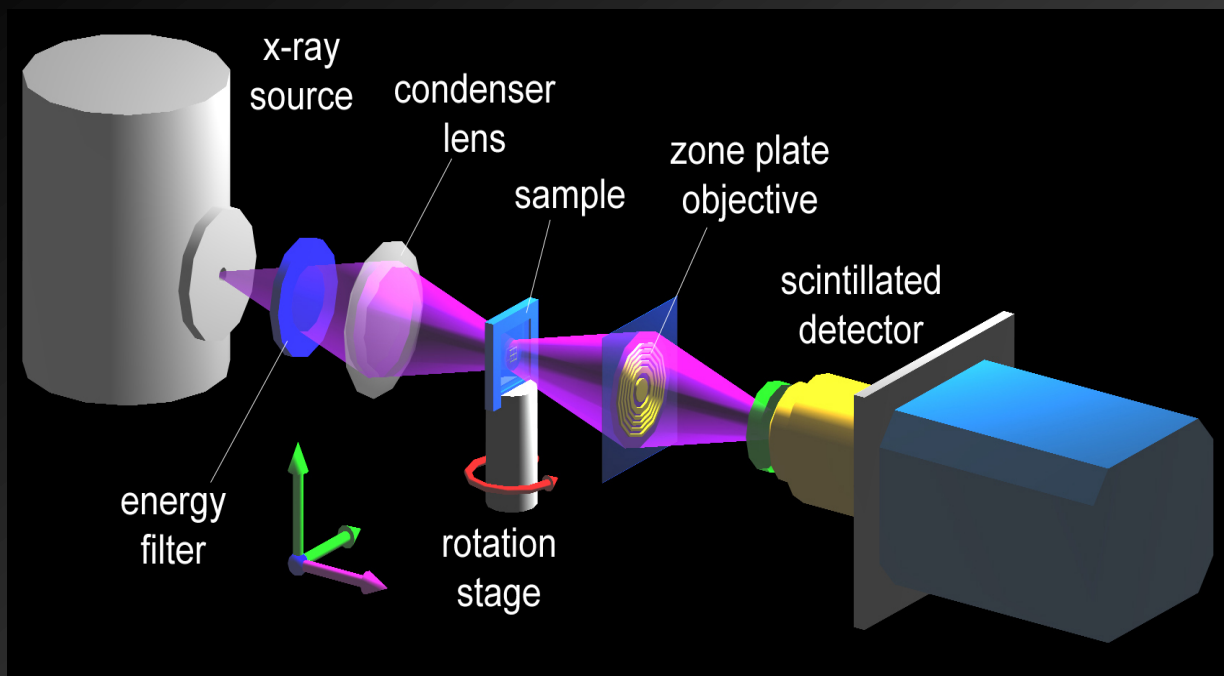


Hard x-ray zone plate microscopy

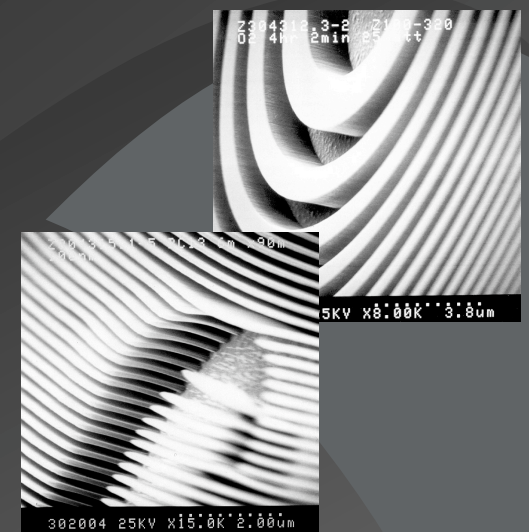


- Shorter wavelengths, potentially better spatial resolution and greater depth-of-field.
- Less absorption (β); phase shift (δ) dominates, higher efficiency.
- Thicker structures required (e.g., zones), higher aspect ratios pose nanofabrication challenges.
- Contrast of nanoscale samples minimal; will require good statistics, uniform background, dose mitigation.

Nanoscale hard x-ray tomography



X-ray Zone-plate Lens



Challenges for achieving nm scale resolution:

- High resolution objective lens: limiting the ultimate resolution
- High numerical aperture condenser lens:
- Detector: high efficiency for lab. source and high speed for synchrotron sources
- Precision mechanical system

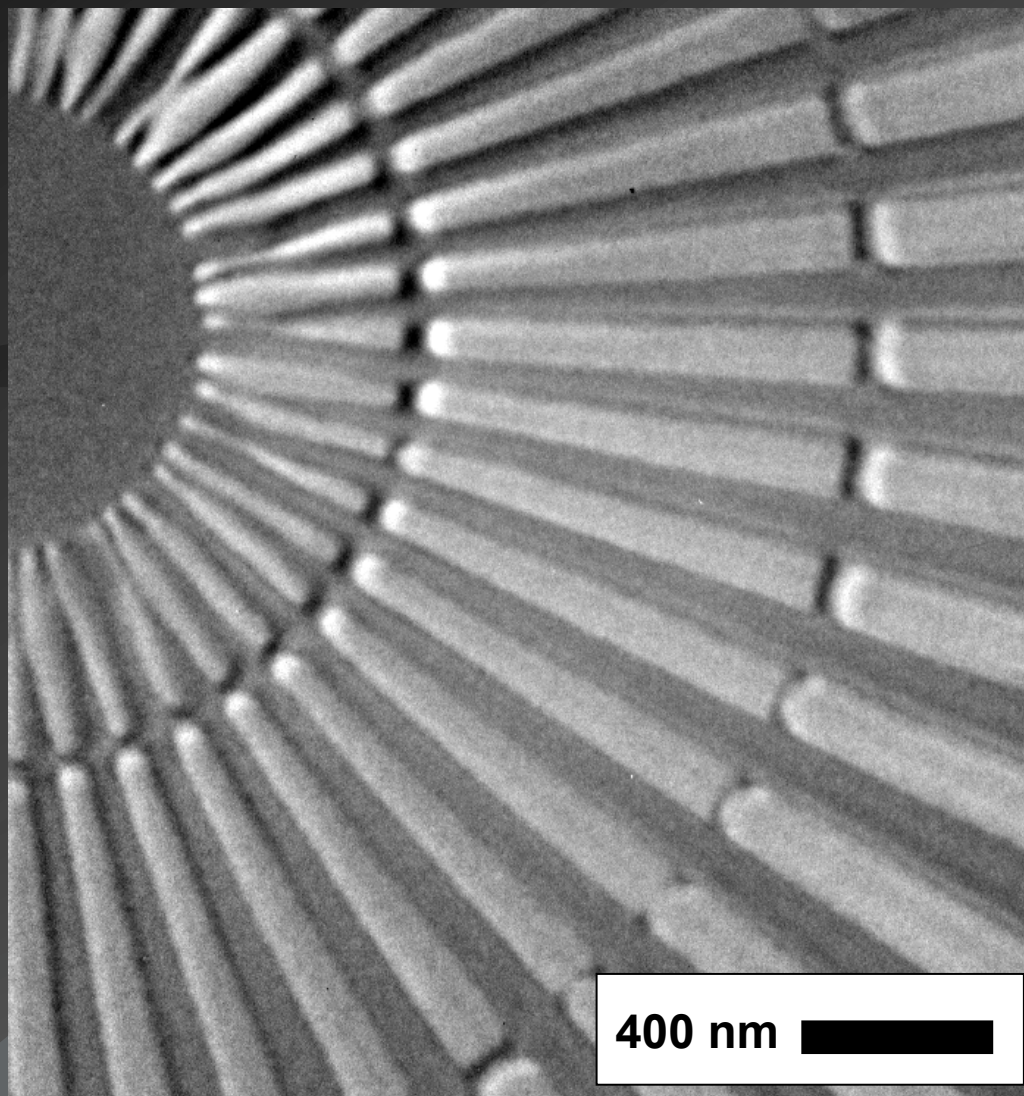
Xradia nanoXCT: Sub-25 nm Hard X-ray Image

Xradia Resolution Pattern

- 50 nm bar width
- 150 nm thick Au
- 8keV x-ray energy
- 3rd diffraction order

F. Duewer, M. Tang,
G. C. Yin, W. Yun,
M. Feser, et al.

Xradia nano-XCT
8-50S installed at
NSRRC, Taiwan

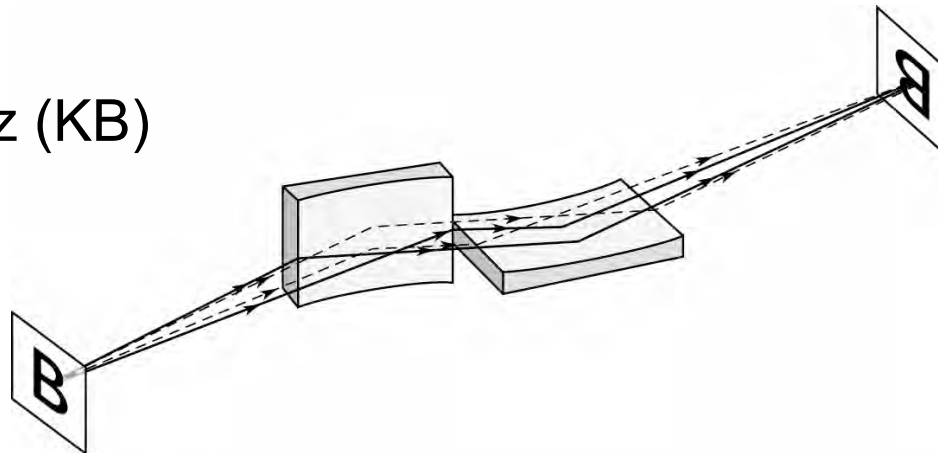




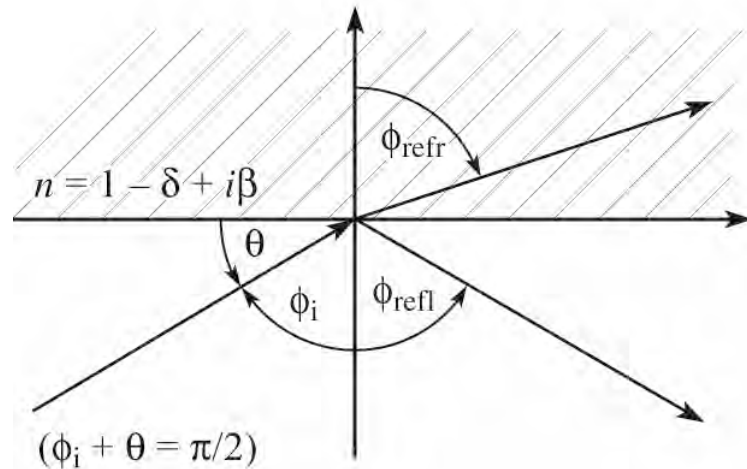
Hard x-ray imaging based on glancing incidence reflective optics



- Optics behave differently at these very short wavelengths (nanometers rather than 520 nm green light)
- The refractive index is less than unity, $n = 1 - \delta + i\beta$
- Waves bend away from the normal at an interface
- Absorption is significant in all materials and at all wavelength.
- Because of absorption, refractive lenses do not work, prisms do not, windows need to be extremely thin (100 nm or less).
- Because light is bent away from the surface normal, it possible to have “total external reflection” at glancing incidence – a commonly used technique.
- Kirkpatrick-Baez (KB) mirror pair



Glancing incidence optics



Snell's Law: $\sin \phi_{\text{refr.}} = \frac{\sin \phi_i}{n}$

Total external Reflection:

$$\phi_{\text{refr.}} \rightarrow \frac{\pi}{2} \text{ as } \phi_i \rightarrow \phi_{\text{critical}}$$

$$\text{Snell's Law: } 1 = \frac{\sin \phi_c}{1 - \delta}$$

$$\sin(90^\circ - \theta_c) = 1 - \delta$$

$$\cos \theta_c = 1 - \delta$$

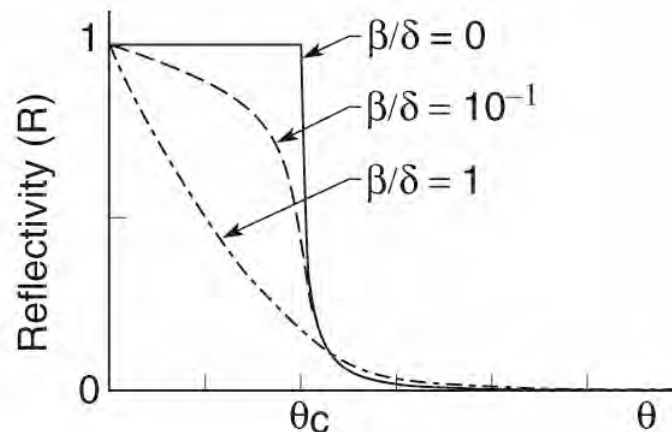
$$1 - \frac{\theta_c^2}{2} = 1 - \delta$$

$$\theta_c = \sqrt{2\delta}$$

For gold at 1 keV

$$\delta = 2.1 \times 10^{-3}$$

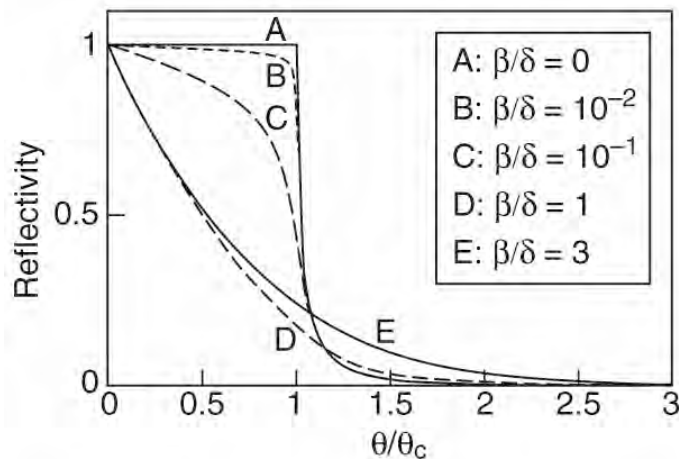
$$\theta_c = 3.7^\circ$$



([www.cxro.LBL.gov](http://www.cxro.lbl.gov) ;
"X-ray properties of the elements"
"X-ray interaction with matter")

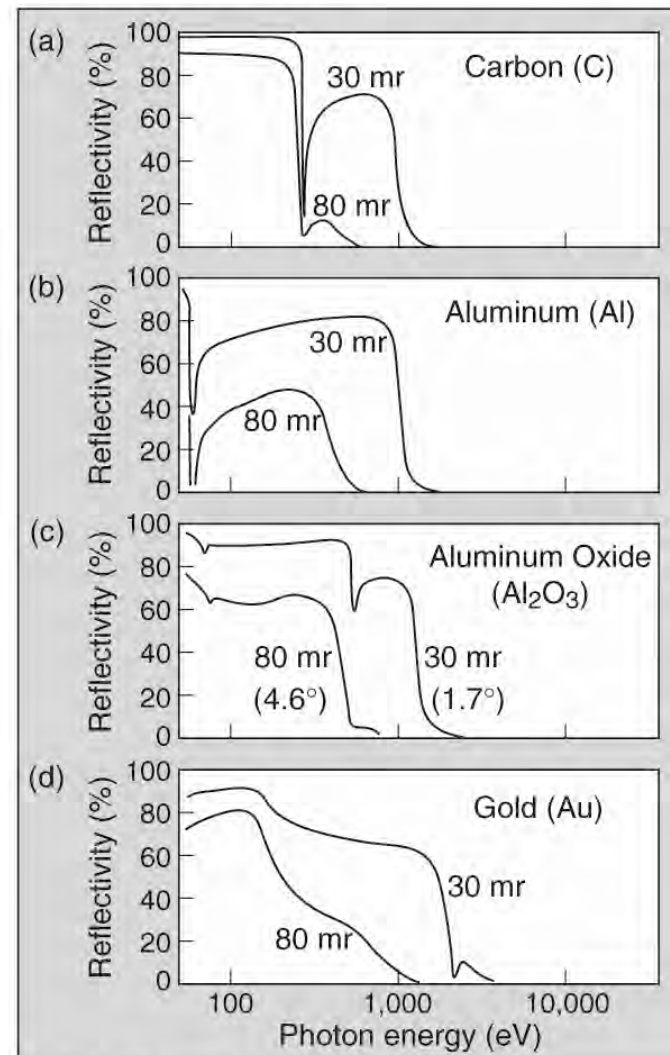
Total external reflection with finite β

Glancing incidence reflection
as a function of β/δ



- finite β/δ rounds the sharp angular dependence
- cutoff angle and absorption edges can enhance the sharpness
- note the effects of oxide layers and surface contamination

... for real materials



(Henke, Gullikson, Davis)

Ch03_TotalExtnlReflec3.ai

Normal incidence reflection at an interface

$$R_s = \frac{|\cos \phi - \sqrt{n^2 - \sin^2 \phi}|^2}{|\cos \phi + \sqrt{n^2 - \sin^2 \phi}|^2} \quad (3.49)$$

at $\phi = 0$:

$$R_{s,\perp} = \frac{|1 - n|^2}{|1 + n|^2} = \frac{(1 - n)(1 - n^*)}{(1 + n)(1 + n^*)}$$

For $n = 1 - \delta + i\beta$

$$R_{s,\perp} = \frac{(\delta - i\beta)(\delta + i\beta)}{(2 - \delta + i\beta)(2 - \delta - i\beta)} = \frac{\delta^2 + \beta^2}{(2 - \delta)^2 + \beta^2}$$

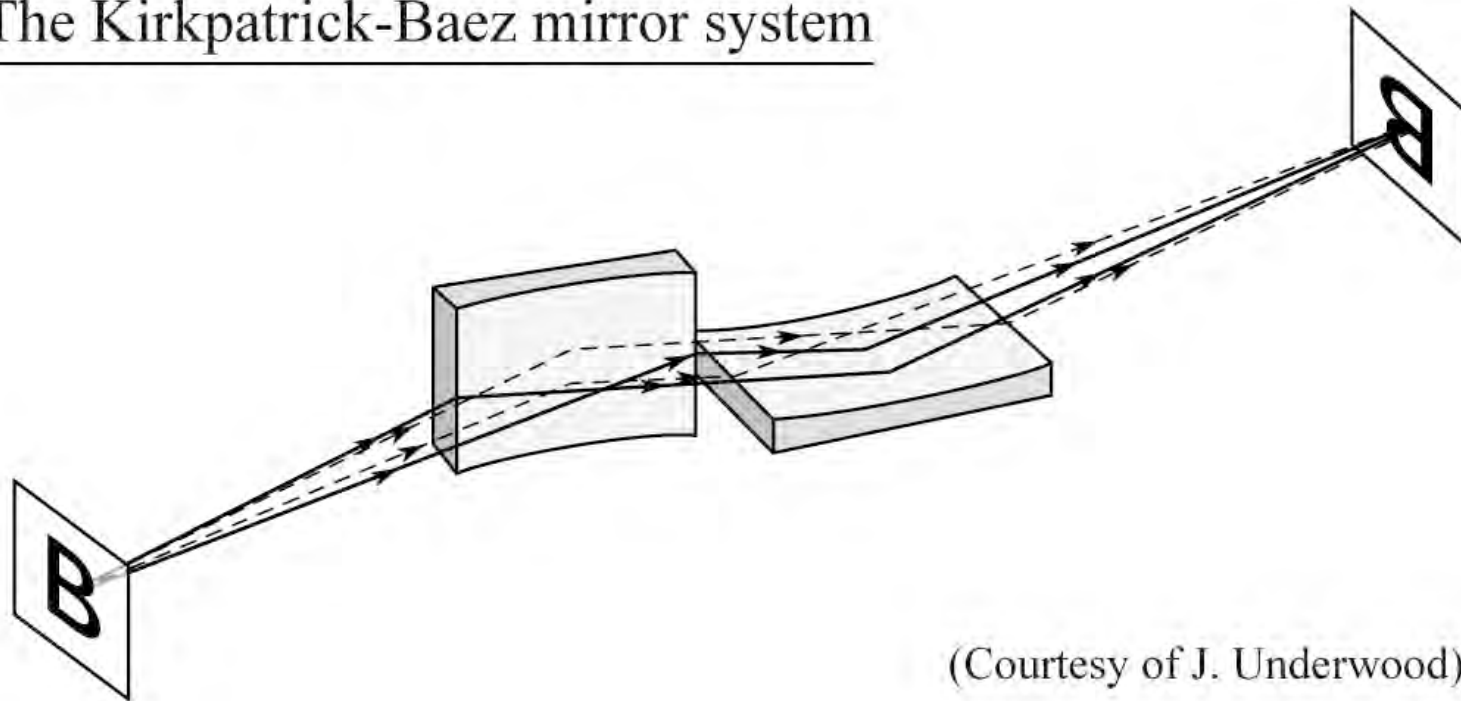
Reflectivity for x-ray and EUV
radiation at normal incidence ($\phi = 0$):

$$R_{s,\perp} \simeq \frac{\delta^2 + \beta^2}{4} \quad (3.50)$$

Example: Nickel @ 300 eV (4.13 nm)

$$\left. \begin{array}{ll} f_1^o = 17.8 & f_2^o = 7.70 \\ \delta = 0.0124 & \beta = 0.00538 \end{array} \right\} R_{\perp} = 4.58 \times 10^{-5}$$

The Kirkpatrick-Baez mirror system

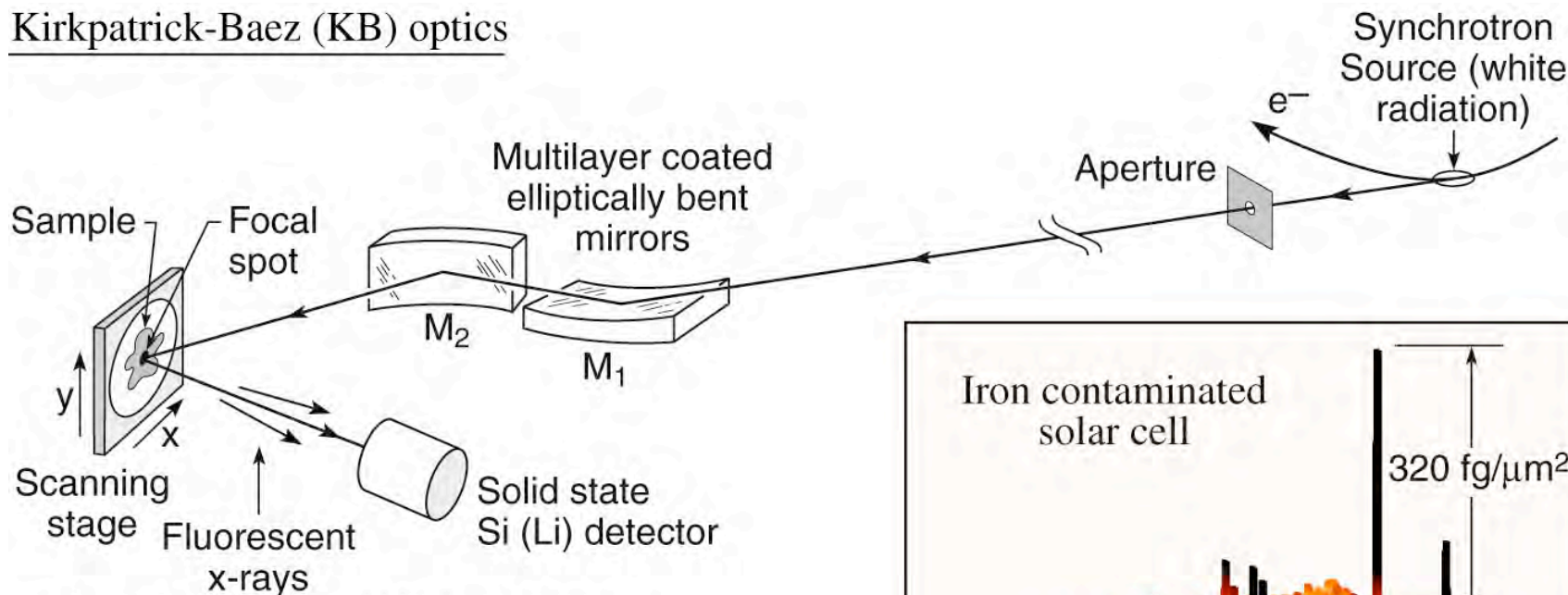


(Courtesy of J. Underwood)

- Two crossed cylinders (or ellipses)
- Astigmatism cancels
- Common use in synchrotron radiation beamlines
- Hard x-ray microprobe

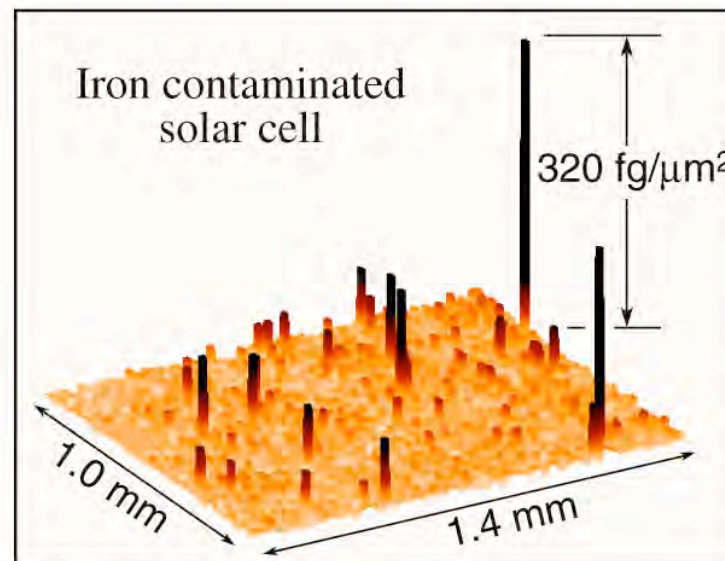
Fluorescent microprobe based in crossed cylinders

Kirkpatrick-Baez (KB) optics

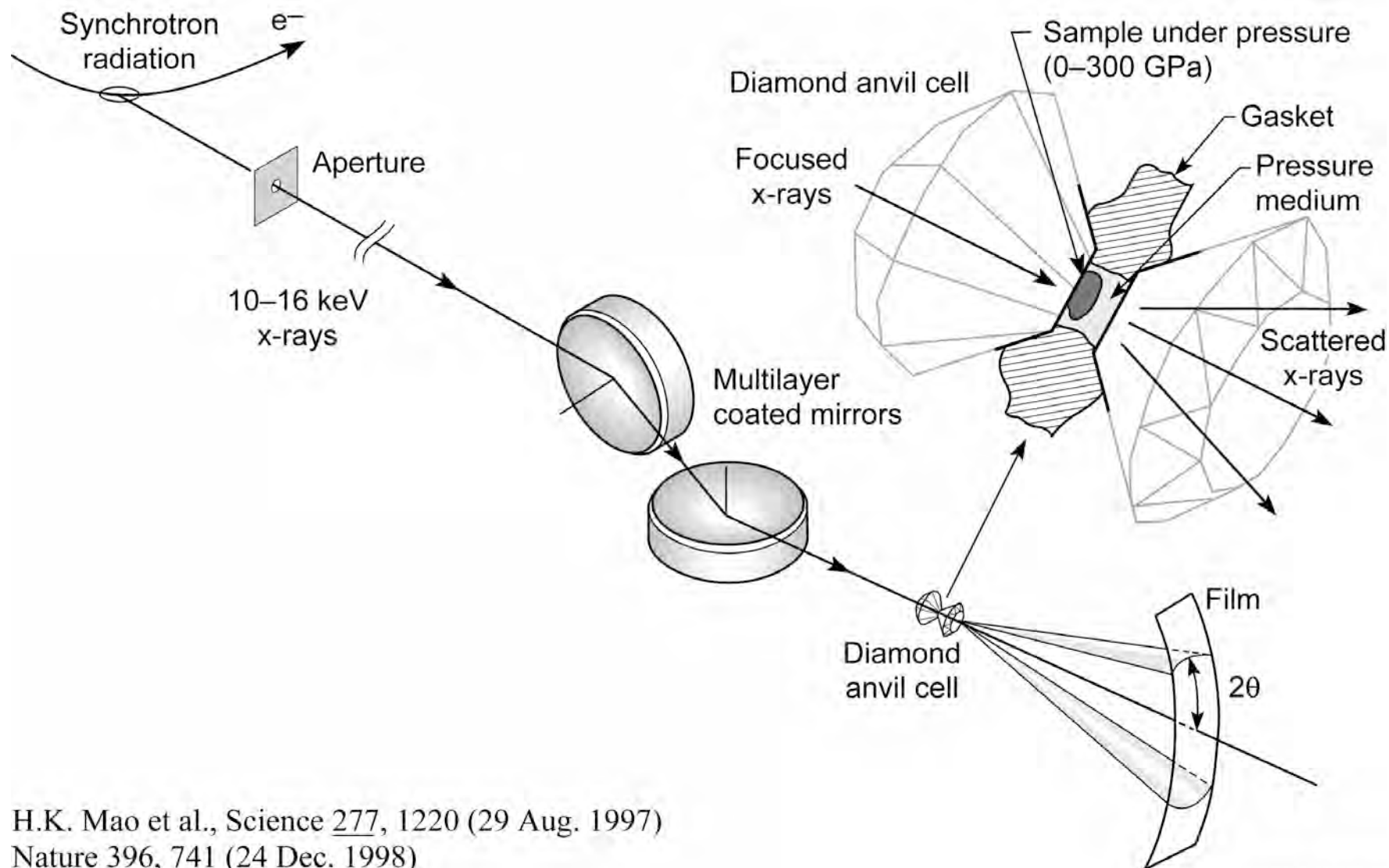


(Courtesy of A. Thompson and J. Underwood, LBNL;
and R. Holm, Miles Lab)

- Crossed cylinders at glancing incidence
- Ellipses better
- Photon in / photon out, low noise background
- Femtogram and part per billion (ppb) sensitivity
- Sub-micron focus (to $0.1 \mu\text{m}$ recently), but scattering gives several micron “50% encircled energy”
- K-B optics have many applications to synchrotron beamlines, fusion diagnostics, etc.



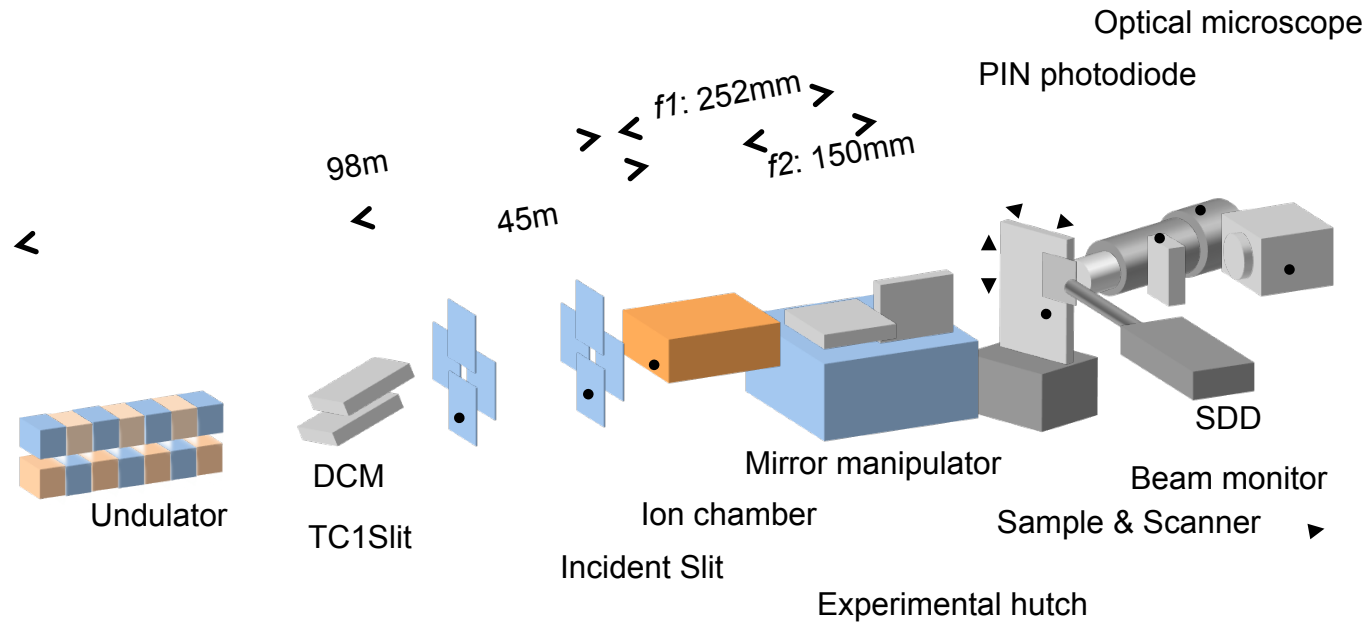
High resolution x-ray diffraction under high pressure using multilayer coated focusing optics



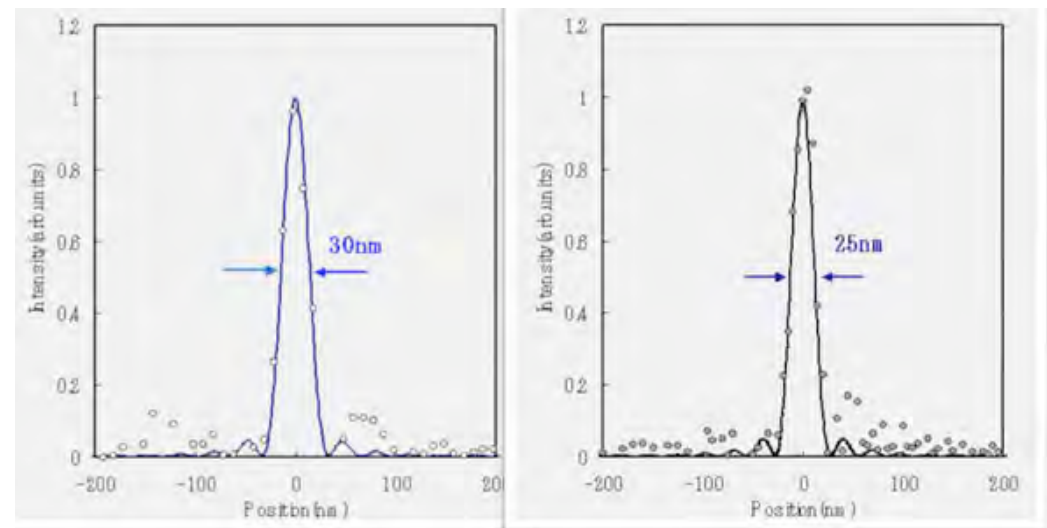
H.K. Mao et al., *Science* **277**, 1220 (29 Aug. 1997)
Nature **396**, 741 (24 Dec. 1998)

Ch04_F16aVG.ai

X-ray microprobe at SPring-8



2006



Courtesy of K. Yamauchi and
H. Mimura, Osaka University.

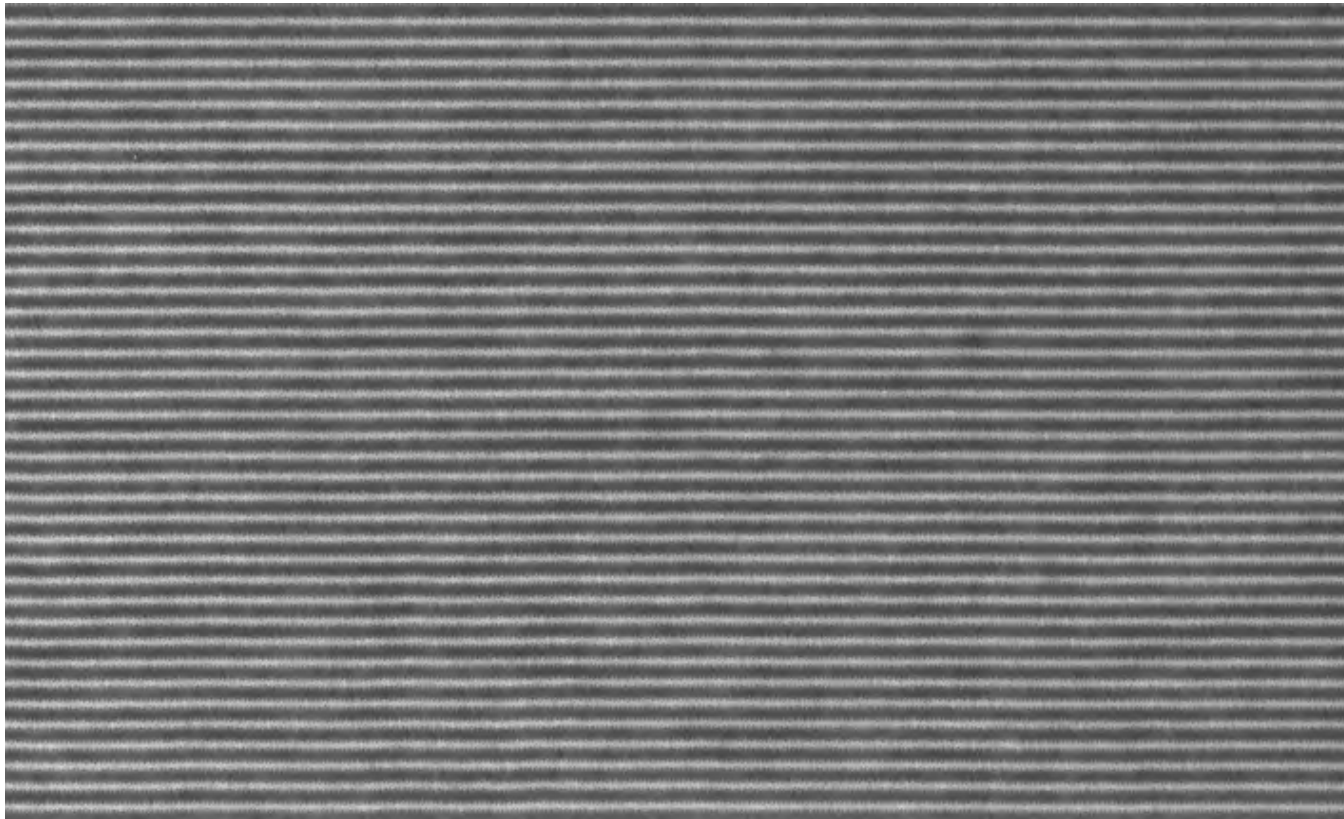


A high quality Mo/Si multilayer mirror



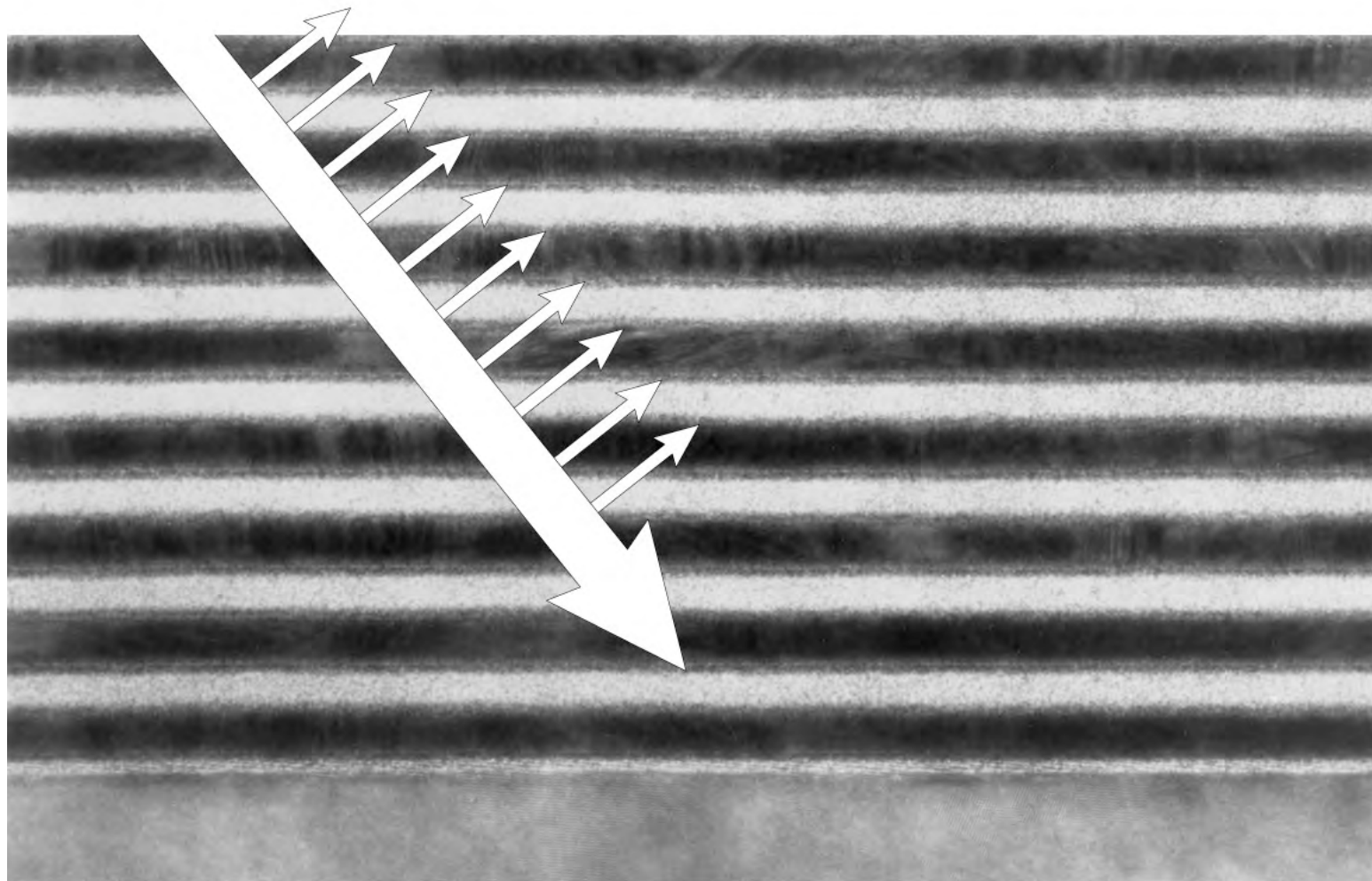
$N = 40$

$d = 6.7$



Courtesy of Saša Bajt (LLNL)

Scattering by density variations within a multilayer coating

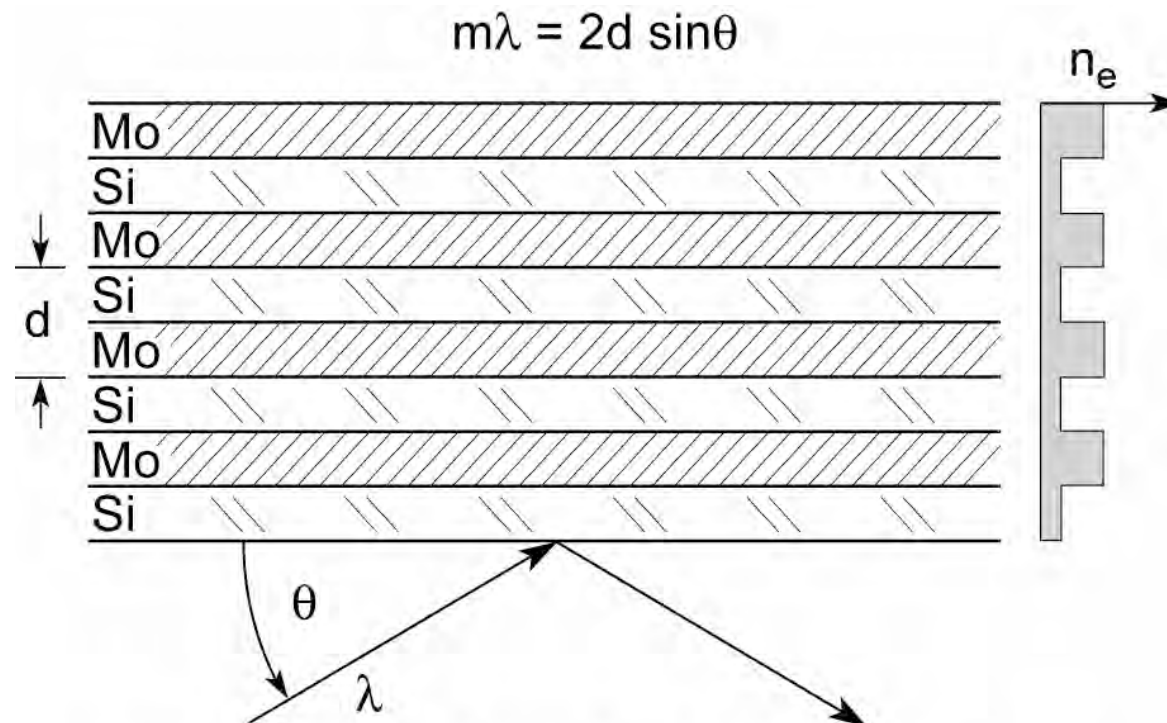


Mo/Si

(T. Nguyen, CXRO/LBNL)

Ch04_F01_Feb2007.ai

Multilayer mirrors satisfy the Bragg condition



For normal incidence, $\theta = \pi/2$, first order ($m = 1$) reflection

$$\lambda = 2d$$

$$d = \lambda/2$$

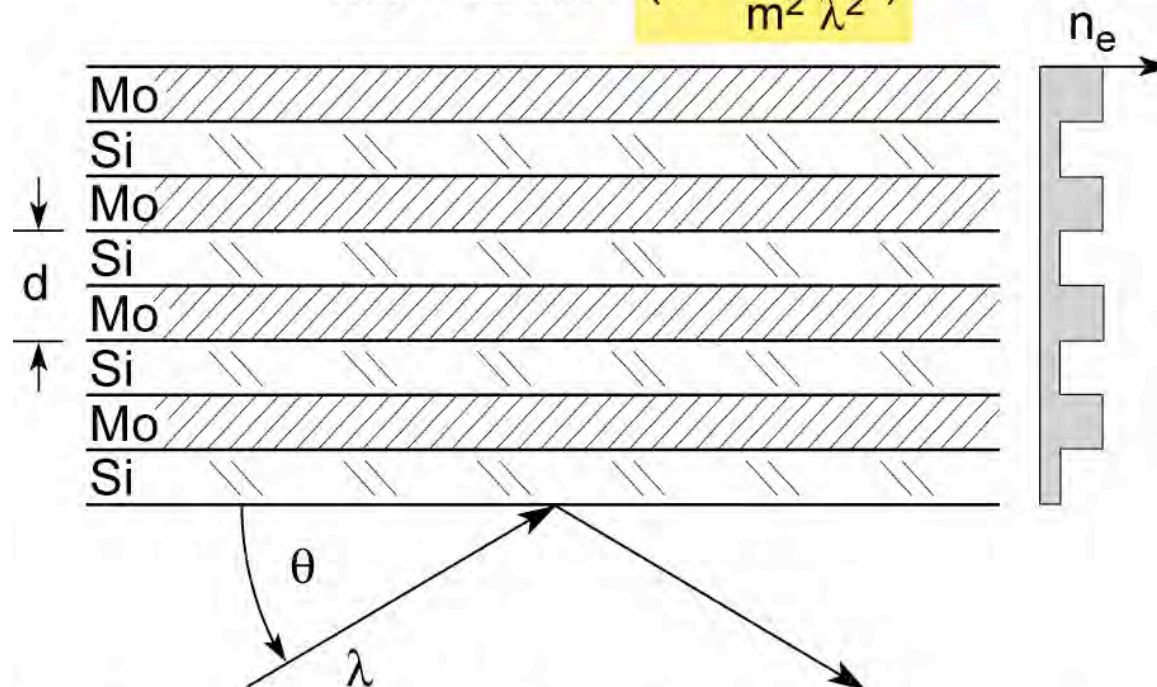
if the two layers are approximately equal

$$\Delta t \approx \lambda/4$$

a quarter-wave plate coating.

Multilayer mirrors satisfy the Bragg condition

$$m\lambda = 2d \sin\theta \left(1 - \frac{4\bar{\delta}d^2}{m^2 \lambda^2}\right)$$



For normal incidence, $\theta = \pi/2$, first order ($m = 1$) reflection

$$\lambda = 2d$$

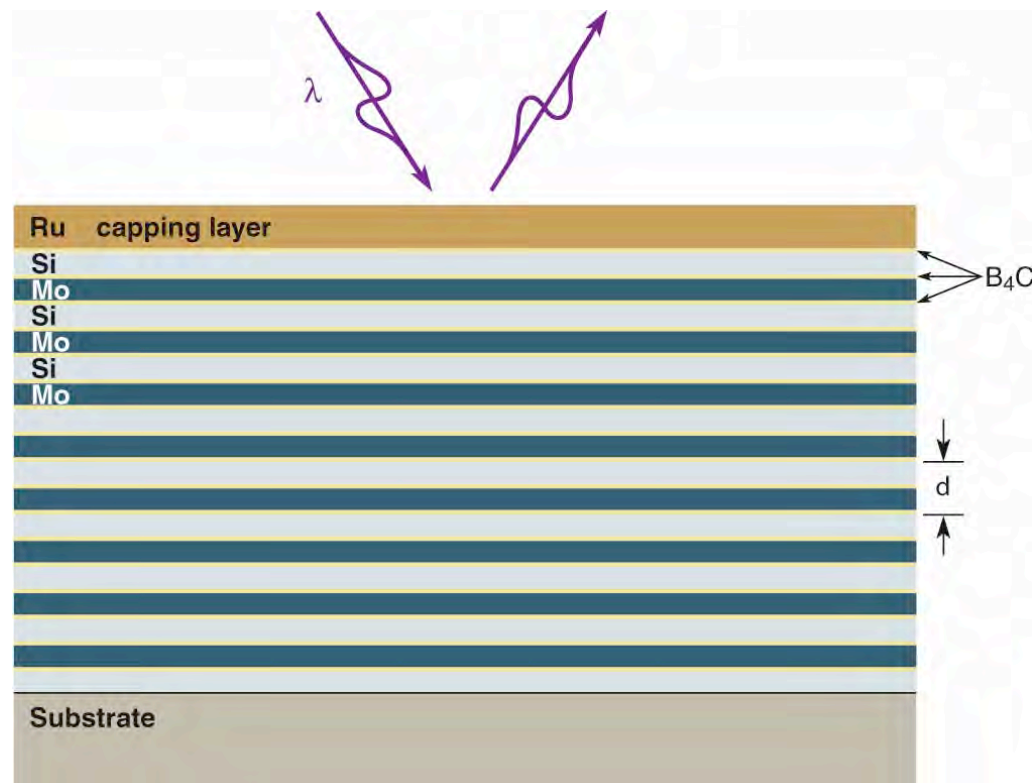
$$d = \lambda/2$$

if the two layers are approximately equal

$$\Delta t \simeq \lambda/4$$

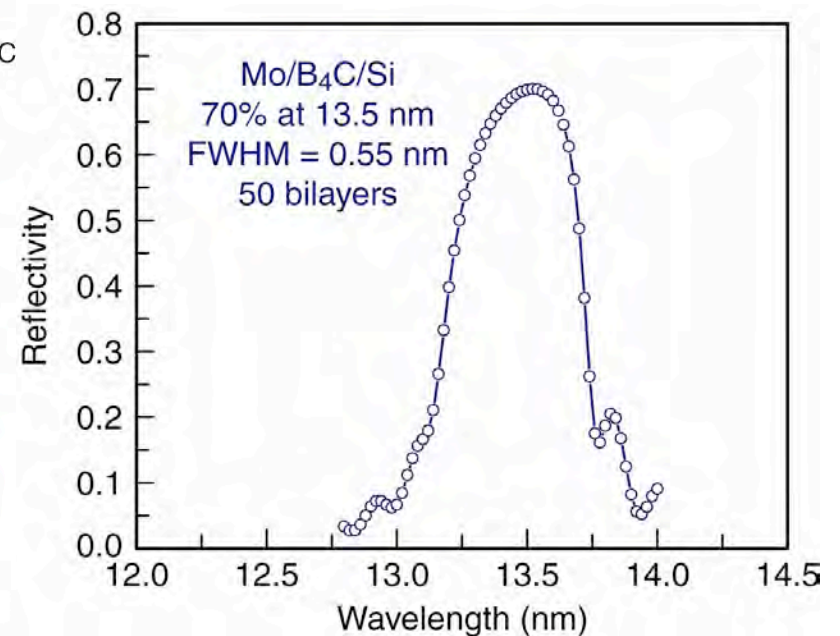
a quarter-wave plate coating.

High reflectivity, thermally and environmentally robust multilayer coatings for high throughput EUV lithography



$\lambda = 13.4 \text{ nm}$

Ru (1.70 nm)	$\left. \begin{array}{l} d = 6.88 \text{ nm} \\ \Gamma = 0.34 \end{array} \right\}$
Si (4.14 nm)	
B ₄ C (0.25 nm)	
Mo (2.09 nm)	
B ₄ C (0.40 nm)	



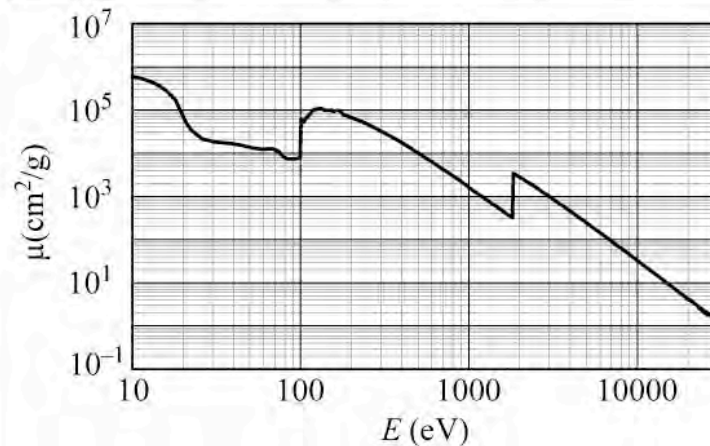
Courtesy of Saša Bajt (LLNL)

Atomic scattering factors for silicon (Z = 14)

$$\sigma_a(\text{barns/atom}) = \mu(\text{cm}^2/\text{g}) \times 46.64$$

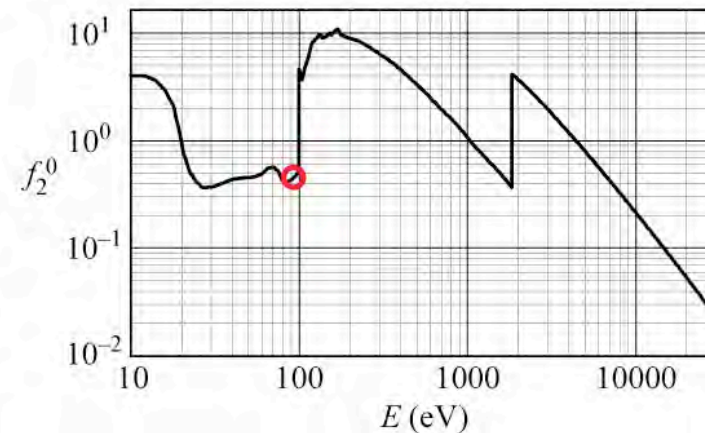
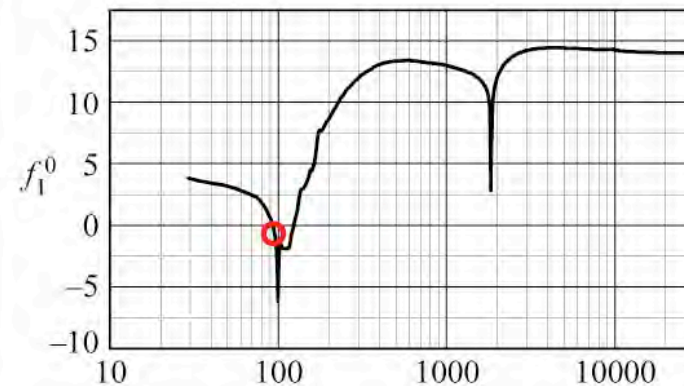
$$E(\text{keV})\mu(\text{cm}^2/\text{g}) = f_2^0 \times 1498.22$$

Energy (eV)	f_1^0	f_2^0	$\mu(\text{cm}^2/\text{g})$
30	3.799	3.734E-01	1.865E+04
70	2.448	5.701E-01	1.220E+04
100	-5.657	4.580E+00	6.862E+04
300	12.00	6.439E+00	3.216E+04
700	13.31	1.951E+00	4.175E+03
1000	13.00	1.070E+00	1.602E+03
3000	14.23	1.961E+00	9.792E+02
7000	14.33	4.240E-01	9.075E+01
10000	14.28	2.135E-01	3.199E+01
30000	14.02	2.285E-02	1.141E+00



Edge Energies: K 1838.9 eV L₁ 149.7 eV
 L₂ 99.8 eV
 L₃ 99.2 eV

Silicon (Si)
Z = 14
 Atomic weight = 28.086



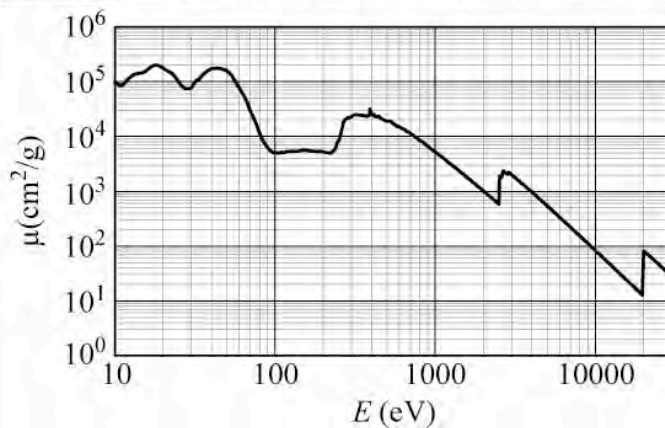
(Henke and Gullikson; www-cxro.lbl.gov)

Atomic scattering factors for molybdenum (Z = 42)

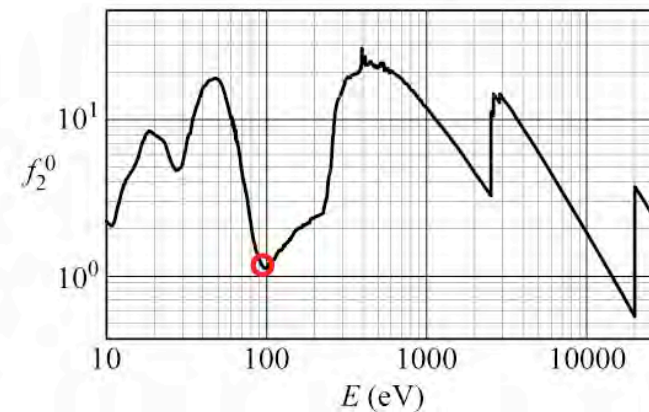
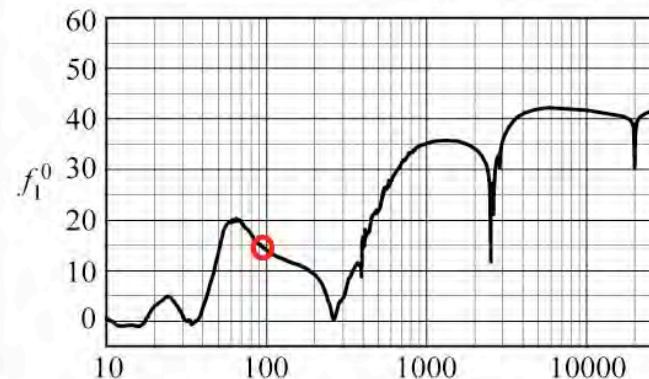
$$\sigma_a(\text{barns/atom}) = \mu(\text{cm}^2/\text{g}) \times 159.31$$

$$E(\text{keV})\mu(\text{cm}^2/\text{g}) = f_2^0 \times 438.59$$

Energy (eV)	f_1^0	f_2^0	$\mu(\text{cm}^2/\text{g})$
30	1.071	5.292E+00	7.736E+04
70	19.38	4.732E+00	2.965E+04
100	14.02	1.124E+00	4.931E+03
300	4.609	1.568E+01	2.292E+04
700	31.41	1.819E+01	1.140E+04
1000	35.15	1.188E+01	5.210E+03
3000	35.88	1.366E+01	1.997E+03
7000	42.11	3.493E+00	2.189E+02
10000	41.67	1.881E+00	8.248E+01
30000	42.04	1.894E+00	2.769E+01



Molybdenum (Mo)
Z = 42
Atomic weight = 95.940



Edge Energies:	K	19999.5 eV	L ₁	2865.5 eV	M ₁	506.3 eV	N ₁	63.2 eV
			L ₂	2625.1 eV	M ₂	411.6 eV	N ₂	37.6 eV
			L ₃	2520.2 eV	M ₃	394.0 eV	N ₃	35.5 eV
					M ₄	231.1 eV		
					M ₅	227.9 eV		


(Henke and Gullikson; www-cxro.lbl.gov)

Ch02ApC_Tb1F12_June2008.ai



CXRO Web Site



CENTER FOR X-RAY OPTICS *Center for X-Ray Optics* 

X-Ray Interactions with Matter . Search CXRO

Facilities

Publications

Research

X-Ray Tools

Visitors

Personnel

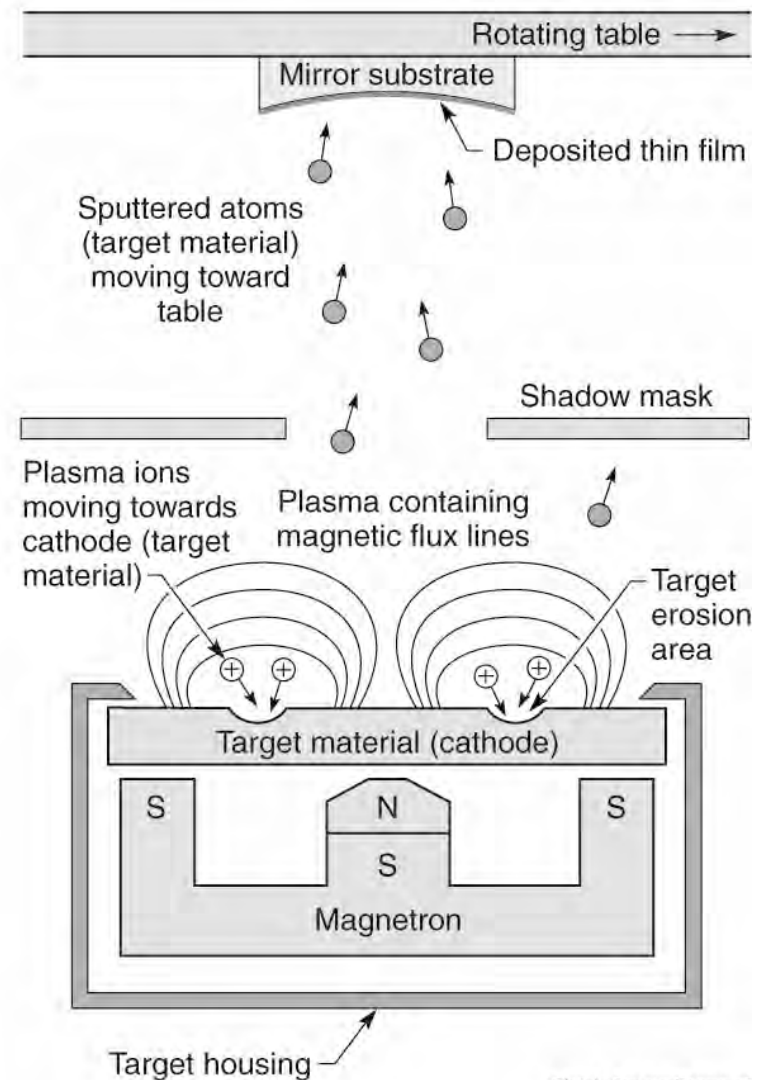
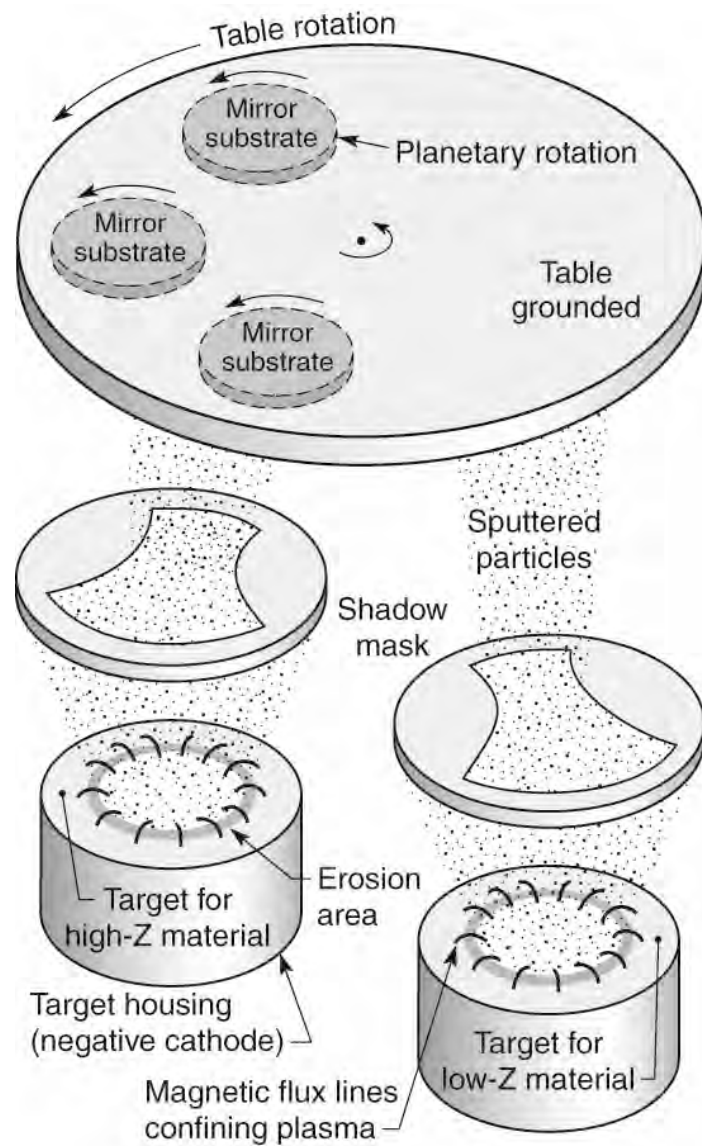
Comments?

Server Stats

www.cxro.LBL.gov/

- **Atomic scattering factors**
- **EUV/x-ray properties of the elements**
- **Index of refraction for compound materials**
- **Absorption, attenuation lengths, transmission**
- **EUV/x-ray reflectivity (mirrors, thin films, multilayers)**
- **Transmission grating efficiencies**
- **Multilayer mirror achievements**
- **Other**

Sputtered deposition of a multilayer coating



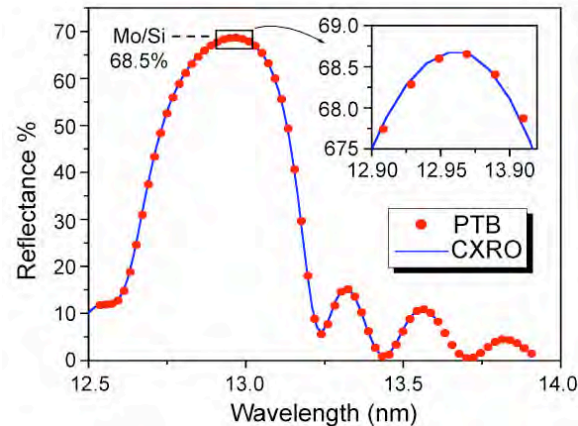
Ch04_SputtrdDepo.ai

Multilayer coatings – “1D nanostructures”

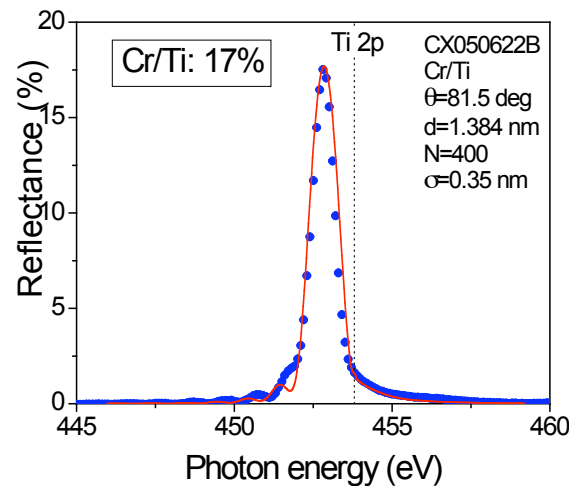
Eric Gullikson, Farhad Salmassi,
Yanwei Liu, Andy Aquila (grad),
Franklin Dollar (UG)



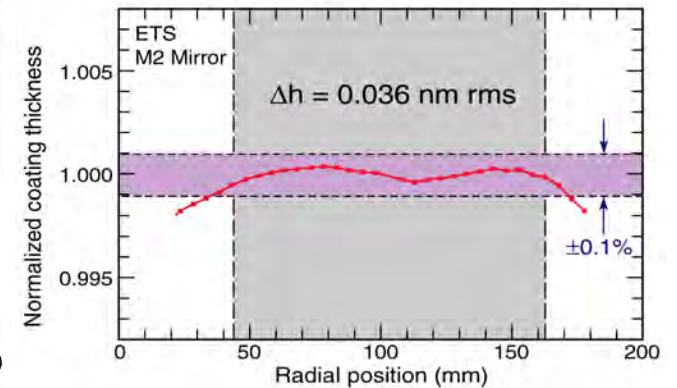
World reference standard



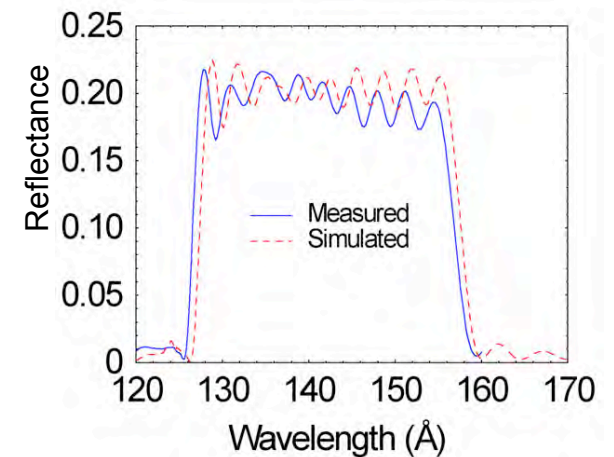
World record in water window



Creating uniformity for $\lambda/50$ optics

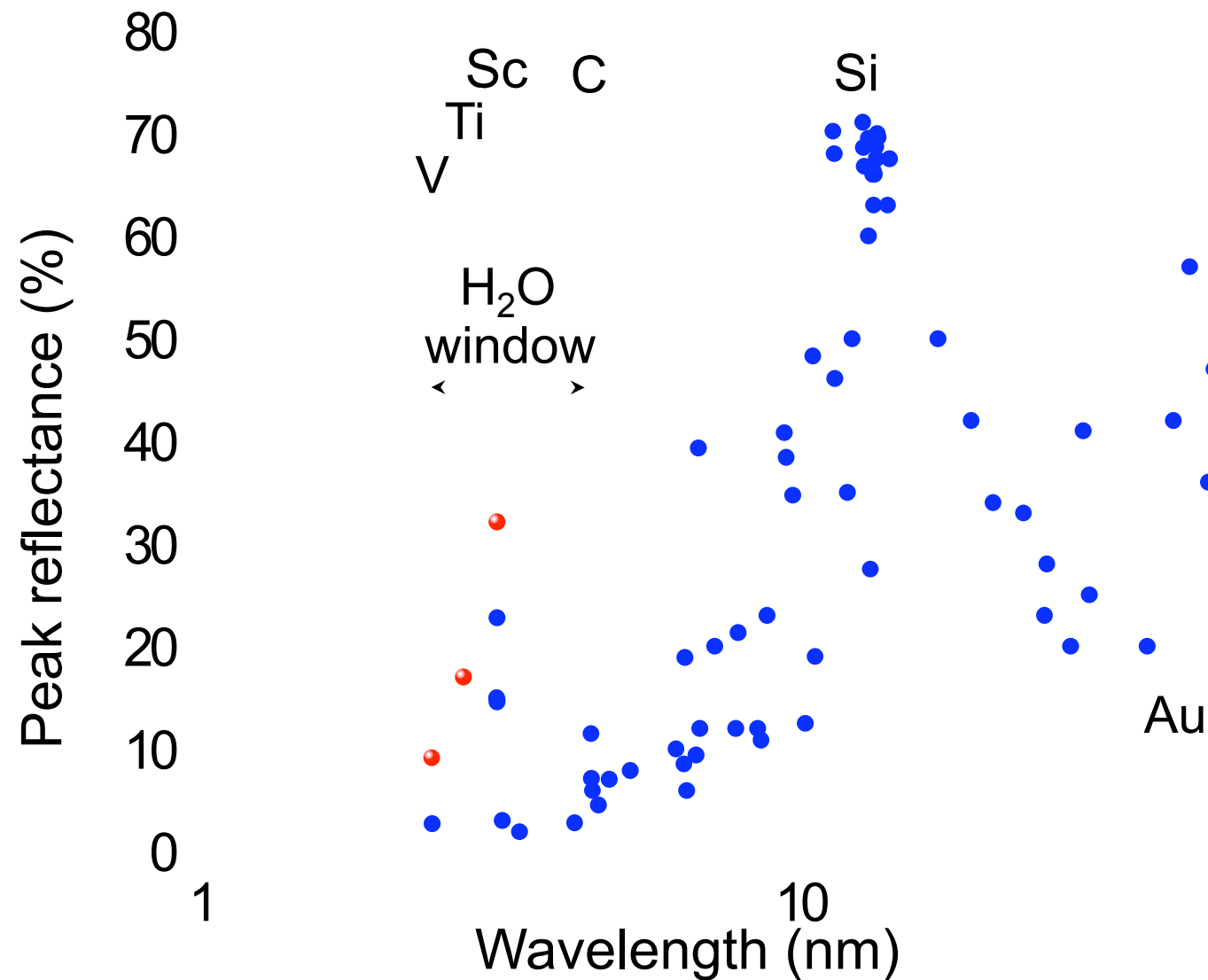


Wide band, narrow band, and chirped mirrors for fsec applications

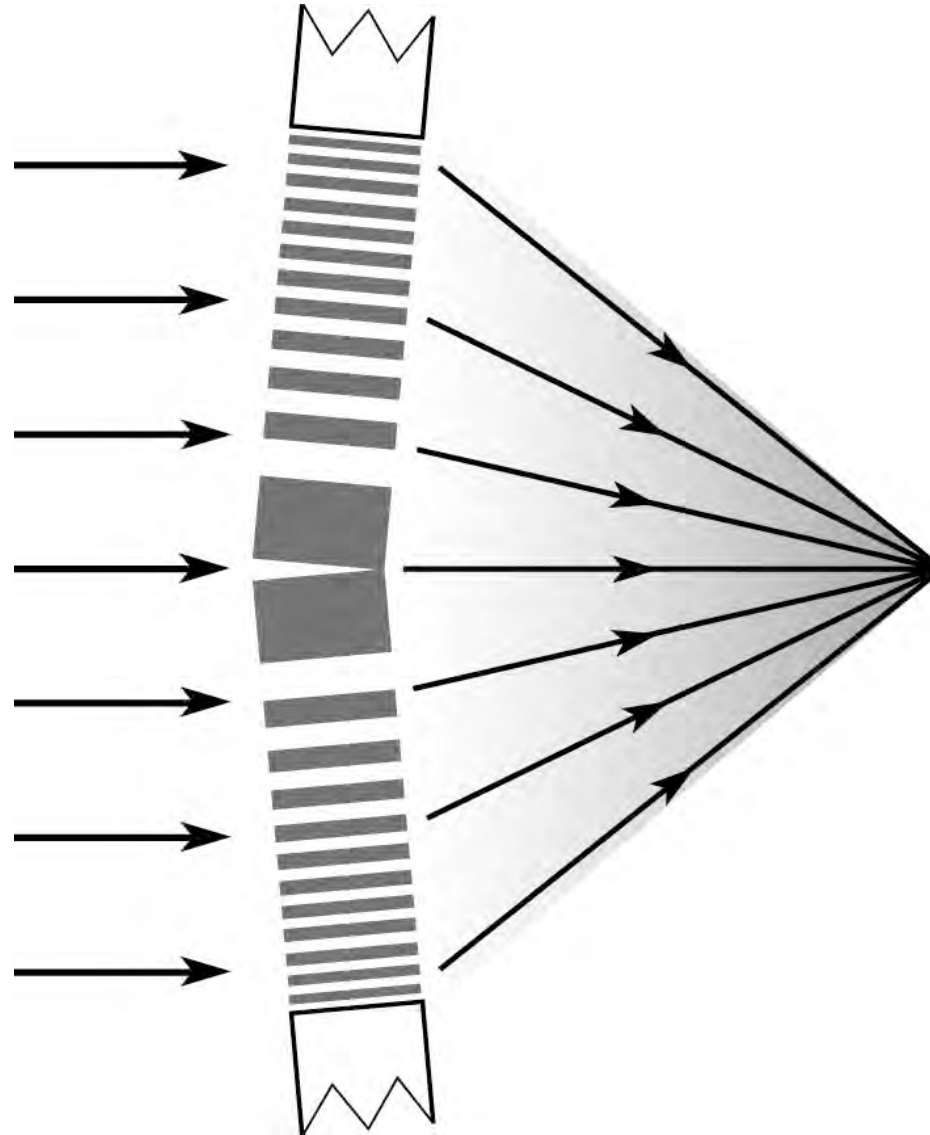


Recent progress in multilayer mirrors

Near-Normal Incidence Multilayer Mirrors

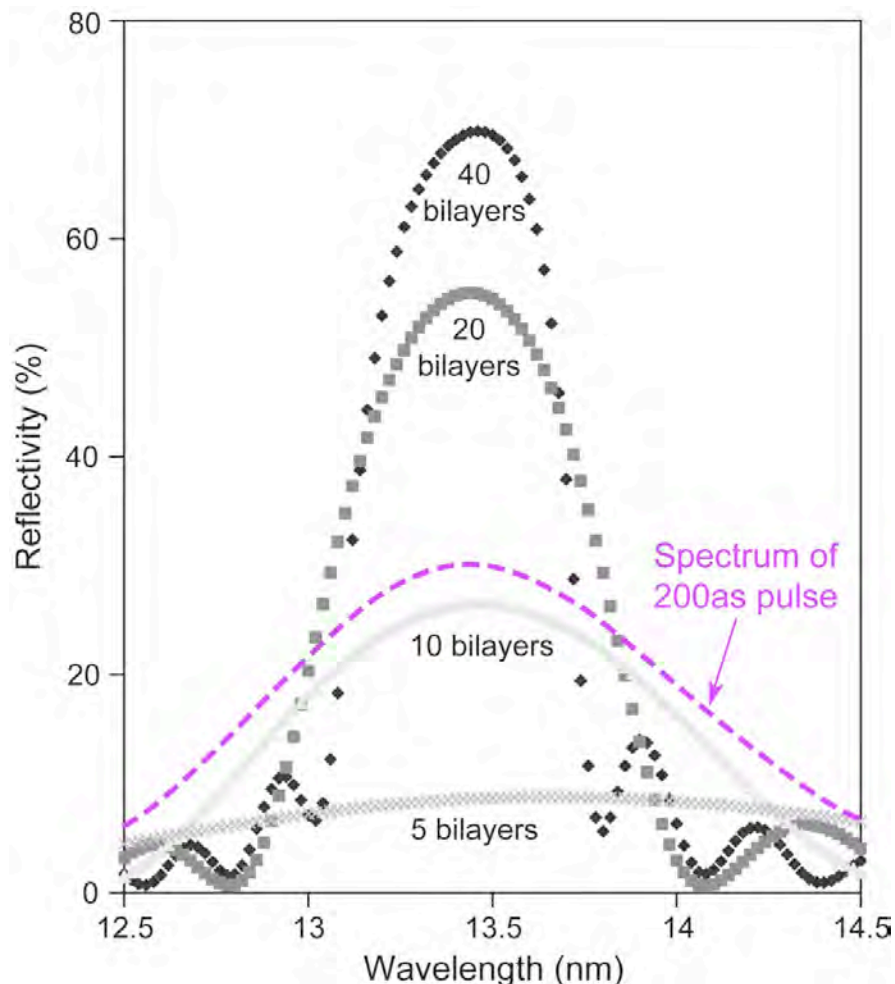


Multilayer Laue Lens for focusing hard x-rays



Broad bandwidth mirrors needed for as/fs pulses

$$\Delta E(\text{eV}) \cdot \Delta \tau(\text{fs}) \geq 1.8 \text{ fs} \cdot \text{eV (FWHM)}$$



- Multilayer mirrors depend on constructive interference from individual interfaces
- Higher reflectivity needs more layers
- Bandwidth gets narrower with more layers

Attosecond pulse

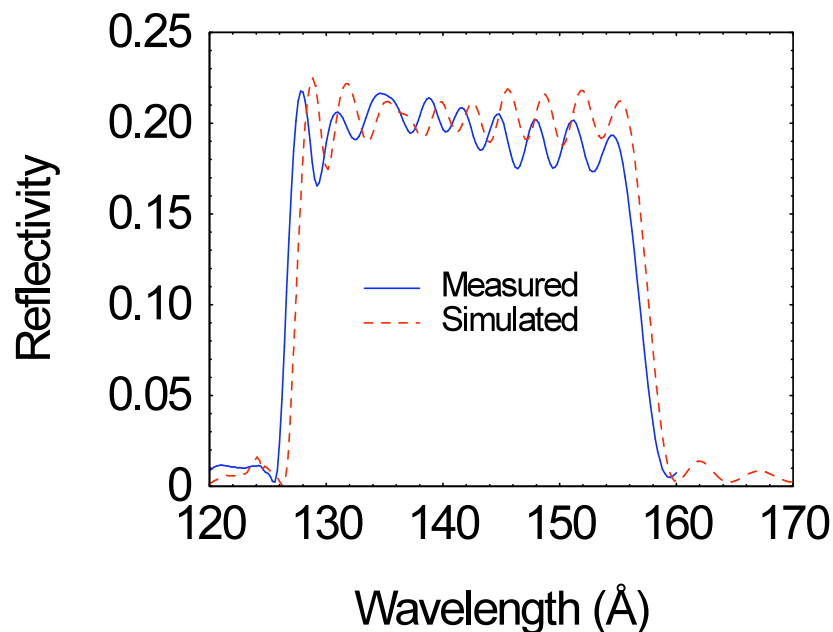
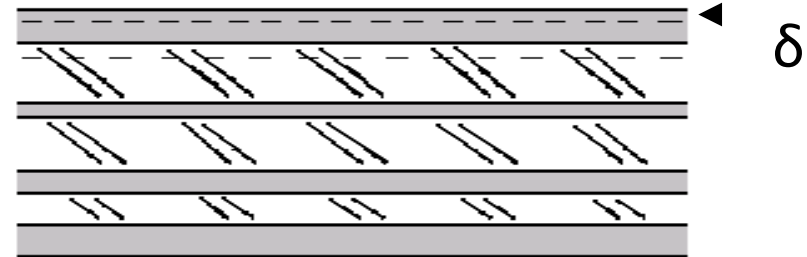
→ Broad bandwidth

→ Limited number of layers

**N<10 layers required for
200 as pulse (@13nm)**

Aperiodic multilayers for asec application

Optimizing multilayers for specific applications requires the use of simulation of a multilayer stack with variations in the thickness of each material in the multilayer.



Successful design of aperiodic multilayers requires:

1. EM wave in multilayer structure
2. Optimization Algorithm
3. Sample preparation
4. Verification

A. L. Aquila, F. Salmasi, F. Dollar, Y. Liu, and E. Gullikson, "Developments in realistic design for aperiodic Mo/Si multilayer mirrors," Opt. Express 14, 10073-10078 (2006)

The Cassegrain Telescope with multilayer coatings for EUV imaging of the solar corona

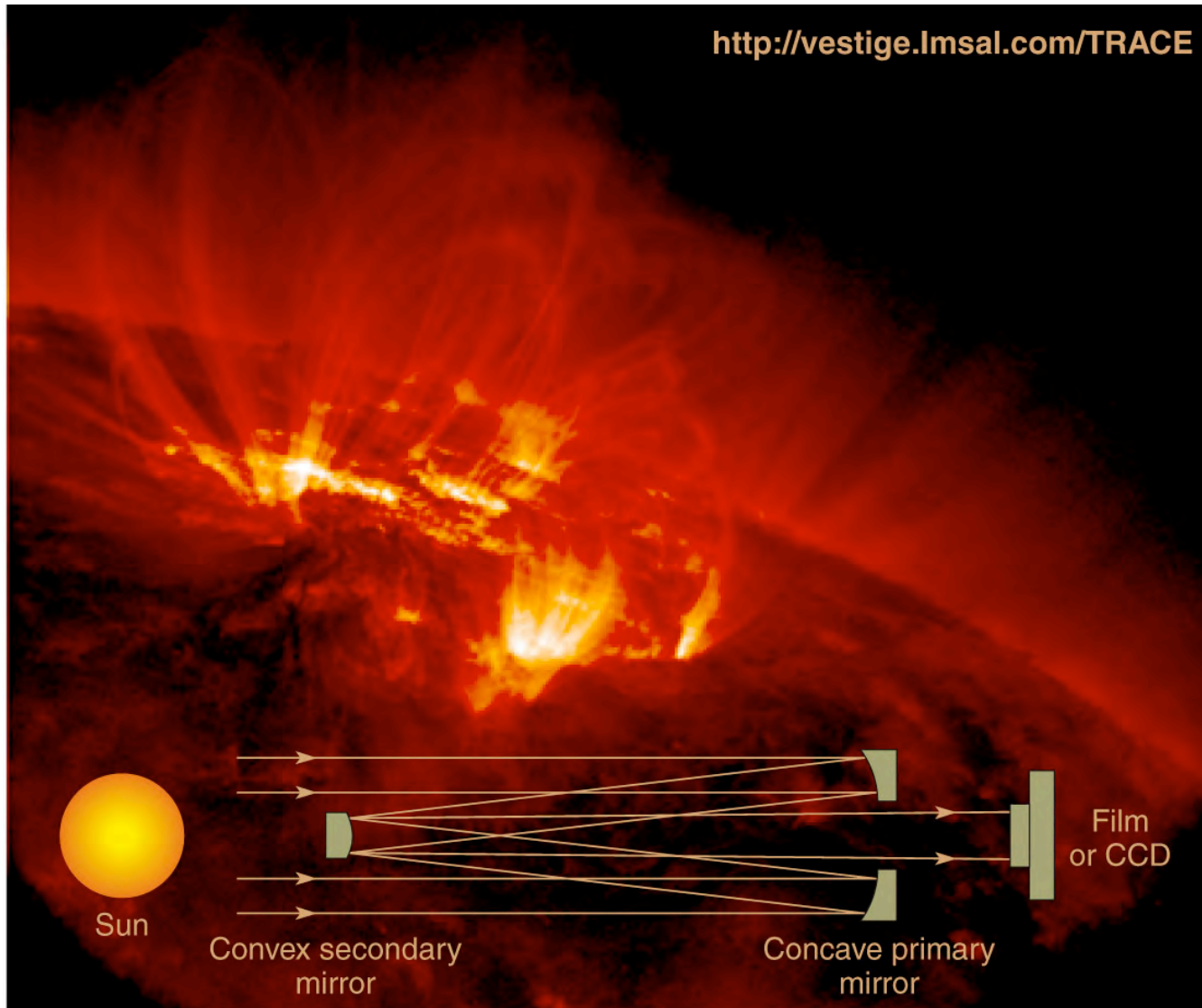


(Photo courtesy of L.Golub, Harvard-Smithsonian and T. Barbee, LLNL)



Photon energy, wavelength, power



$$\hbar\omega \cdot \lambda = hc = 1239.842 \text{ eV nm} \quad (1.1)$$

$$1 \text{ joule} \Rightarrow 5.034 \times 10^{15} \lambda[\text{nm}] \text{ photons} \quad (1.2a)$$

$$1 \text{ watt} \Rightarrow 5.034 \times 10^{15} \lambda[\text{nm}] \frac{\text{photons}}{\text{s}} \quad (1.2b)$$

Ch01_Eqs1.1_2.ai

Refractive index in the soft x-ray and EUV spectral region

$$n(\omega) = 1 - \frac{1}{2} \frac{e^2 n_a}{\epsilon_0 m} \sum_s \frac{g_s}{(\omega^2 - \omega_s^2) + i\gamma\omega} \quad (3.8)$$

Noting that

$$r_e = \frac{e^2}{4\pi\epsilon_0 m c^2}$$

and that for forward scattering

$$f^0(\omega) = \sum_s \frac{g_s \omega^2}{\omega^2 - \omega_s^2 + i\gamma\omega}$$

where this has complex components

$$f^0(\omega) = f_1^0(\omega) - i f_2^0(\omega)$$

The refractive index can then be written as

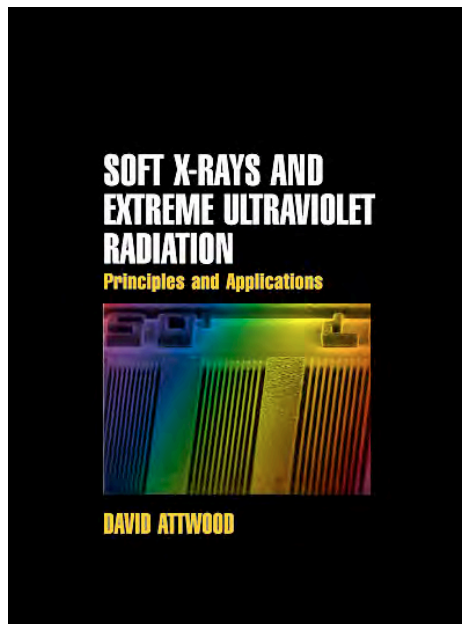
$$n(\omega) = 1 - \frac{n_a r_e \lambda^2}{2\pi} [f_1^0(\omega) - i f_2^0(\omega)] \quad (3.9)$$

which we write in the simplified form

$$n(\omega) = 1 - \delta + i\beta \quad (3.12)$$



Lectures online at www.youtube.com



Amazon.com



UC Berkeley

www.coe.berkeley.edu/AST/sxreuv

www.coe.berkeley.edu/AST/srms

www.coe.berkeley.edu/AST/sxr2009